HEAVY METALS REMOVAL FROM ACID MINE DRAINAGE USING BANANA PEELS

Jan Mbongeni Mahlangu

(0611852N)

A dissertation submitted to the Faculty of Engineering and the Built Environment, University of the Witwatersrand, Johannesburg, in fulfilment of the requirements for the degree of Master of Science in Chemical Engineering.

03 May 2018

Declaration

I declare that, this dissertation is my own work. It is being submitted for the degree of Master of Science in Engineering to the University of the Witwatersrand, Johannesburg. It has not been submitted before for any degree or examination in any other university.

Jan Mbongeni Mahlangu 03 May 2018

Signed:…….

ABSTRACT

The sustainable removal of heavy metals from acid mine drainage (AMD) and wastewater has become a major challenge to scientists (Hossain et al., 2012), despite numerous treatment technologies. Most of the explored technologies cannot remove pollutants completely and others are too expensive and also have significant disposal challenges (Giwa et al., 2013). The need to develop a more effective and affordable technology for the removal of heavy metals from AMD is, therefore, inevitable.

The banana fruit, the most abundant fruit that is almost consumed across the world its peels were explored to study their potential to remove heavy metals under AMD conditions.
The banana peels were cut, washed, dried and ground into powder. Thereafter, the adsorption of zinc, copper and manganese metal ions were studied to investigate the effects of controlling parameters such as particle size, adsorbent dose, initial heavy metal ion concentration, contact time, pH and selectivity of the banana peel. Synthetic single- and ternary component solution, fortified AMD and actual AMD were used in a batch system. Langmuir and Freundlich isotherms were applied to describe adsorption equilibrium. The maximum amount of zinc, copper and manganese metal ions adsorbed, as evaluated by Langmuir isotherm were 9.017, 8.718 and 6.920 mg/g, respectively. The adsorption data fitted the pseudo second order very well and suggested that the adsorption is characterized by the valence forces through exchange of charges between banana peel powder and heavy metal ions.

Continuous fixed bed column studies were conducted by using AMD at room temperature and the effects of various parameters such as flow rate (15, 30 and 45 mL/min) and bed depths (6, 12.4 and 17.8 cm) were investigated. The column bed capacity and saturation time increased with the increase of bed depth and decrease of flow rate. Furthermore, the results show that the column performed well at the lowest flow rate. The Thomas model and bed depth service time (BDST) model were applied to evaluate the breakthrough curves and to analyse the experimental data. Thomas model showed a consistent low level of regression coefficient, R^2; 0.240 and 0.738 for Mn metal ion at bed depth of 6 cm and 17 cm and flowrate of 15 ml/min, respectively and 0.709 and 0.649 for Zn metal ion at bed depth of 6 cm and 17 cm and flowrate of 15 ml/min, respectively. It can be concluded that the experimental data did not fit well with this model. The BDST model showed adsorption of 150.759 and 27.722 mg/g for manganese and zinc, respectively.

The results obtained in this study demonstrated that the banana peel powder can be used as an adsorbent for the removal of zinc, copper and manganese metal ions from AMD using batch and fixed bed adsorption system.

Dedication

I would like to dedicate this work to my wife Thandiwe Masombuka, my daughter Hlelolwethu Mahlangu and the coming generations of scientists and engineers who will find this work useful.

Acknowledgements

I would like to thank my father in heaven, God the Almighty for the strength He provided me with.

I would like to thank my supervisors, Prof G S Simate and Dr M de Beer for their dedicated supervision, insight into this research topic, useful ideas and advice.

Furthermore, I would like to thank my colleagues with different technical expertise who assisted: Popoti Maake (ICP MS), Solly Motaung (BET), Sharon Eggers (SEM) and Lindo Mdletshe (FTIR).

Finally, my wife Thandiwe Masombuka for understanding when I had little time for us and my daughter Hlelolwethu Mahlangu, daddy was not always there for you but you were too young to understand.

TABLE OF CONTENTS

LIST OF FIGURES

LIST OF TABLES

APPENDIX A

APPENDIX B

GLOSSARY

AMD	Acid mine drainage
Zn	Zinc ion
Cu	Copper ion
Mn	Manganese ion
Al	Aluminium ion
Cd	Cadmium ion
Co	Cobalt ion
Ni	Nickel
Fe	Iron III ion
ICP-MS	Inductively-Coupled Plasma Mass Spectroscopy
SEM	Scanning Electron Microscopy
FTIR	Fourier Transform Infrared Spectroscopy
N_2-BET	Nitrogen Brunauer-Emmett-Teller

CHAPTER 1

1.1 Introduction

One very well-known pollution problem emanating from current and historical mining activities globally and South Africa, in particular, is termed acid mine drainage (AMD) (Simate and Ndlovu, 2014).South Africa is one of the leaders in mining in the world, and the country is known for its plentiful mineral resources, which account for a significant proportion of world production and reserves. In addition, South African mining companies play a significant role in global economy and about 25% of South Africa's GDP is derived from mining activities (Stilwell et al., 2000).

However these mining activities degrades water resources due to their release of heavy metals. Moreover, if remedial actions are not taken, water quality can be expected to continue to deteriorate (Ashton et al., 2001). In fact the degradation of water resources is a major environmental problem that the world is facing today. The degradation of water resources leads to ecological damages, and water being a scarce resource in South Africa it is, thus, necessary to protect it.

The inter-ministerial committee released a report on AMD, in December 2010, stating that AMD is a national crisis. The report also emphasized that if no action is taken to decant and treat the AMD, South Africa's main river systems will be greatly affected. The report added that AMD has begun to erode dolomite structures in Johannesburg and near East Rand, and shortly thereafter the water will poison boreholes and fountains as has been happening on the West Rand in the Cradle of human kind, the Krugersdorp Game Reserve and Sterkfontein caves since September 2002 (McCarthy, 2010).

The AMD is polluted water that results when sulphur-bearing minerals associated with coal and gold mining are exposed to air and water (Werdmuller, 1986). Due to its acidity, the mine drainage also dissolves heavy metals from other minerals resulting in acidic and toxic waste streams. Unfortunately, whenever toxic heavy metals are exposed to the natural eco-system, accumulation of metal ion in human bodies will occur through either direct intake or food

chains. Therefore, heavy metals should be prevented from reaching the water bodies (Meena et al., 2008).

Traditionally, AMD has been treated through the precipitation method by increasing its pH with limestone ($CaCO_3$) (Jennings, 2000). However, this method generates high volumes of gypsum ($CaSO_4$) sludge that has disposal challenges. Other conventional methods have also shown to be prohibitively expensive and ineffective (Johnson and Hallberg, 2005). In view of many disadvantages of conventional processes, it is imperative that new methods with exceptional qualities are found.

One such alternative technique that has attracted a lot of attention in recent years is adsorption using agricultural waste. Utilization of cheap natural agricultural waste that is in abundant for the removal of contaminants from aqueous solutions is very economical compared to other physicochemical processes (Marvrov, 2006). Indeed, plant wastes are used as adsorbent worldwide for wastewater treatment (Montanher et al., 2005). One such agricultural plant of interest is the banana. Banana is one of the most widespread fruits in the world and its benefits are not only edible, but its peel has shown a capability of removing heavy metals at significant capacity (Al-Azzawi et al., 2013).

1.2 Problem Statement

The sustainable removal of heavy metals from AMD and wastewater has become a major challenge to scientists (Hossain et al., 2012), despite the fact that numerous treatment technologies such as flocculation, oxidation process, reverse osmosis, chemical precipitation, ion exchange and the use of activated carbon have been explored for the removal of heavy metals from aqueous solutions (Gunatilake, 2015). Nevertheless, most of these technologies cannot remove heavy metal pollutants completely and others are too expensive and also have significant disposal challenges (Giwa et al., 2013). Therefore, a need to develop more effective and affordable technologies for the removal of heavy metals from AMD is inevitable. One such alternative technique that has attracted a lot of attention in recent years is adsorption using agricultural waste, in particular, banana peel waste.

Banana peel is discarded all over the world as a no value material. As a result, it contributes to waste management problems though it has some compost and adsorbent potential. In fact, it is

an abandoned, but readily available low cost environmental friendly bio-material. Indeed, the use of banana peels as an adsorbent material has a strong potential due to its high contentment of cellulose, hemicellulose, lignin and carboxylic groups that can adsorb heavy metals from the solution to the surface.

The proposed study, therefore, aims to answer the following questions:

- Can banana peel remove heavy metals under AMD conditions?
- To what extent can the banana peels remove heavy metals in AMD?

1.3 Research objective

The main aim of the study is to explore the adsorption potential of banana peel as low cost adsorbent for heavy metals from synthetic water, actual AMD and fortified AMD, with manganese (Mn), copper (Cu) and zinc (Zn) being the main targeted heavy metals for the study. The specific objectives are:

- To determine the adsorption capacity of the banana peel waste adsorbent.
- To investigate the effect of pH, contact time, initial heavy metal concentration, adsorbent mass and particle size of the adsorbent on the treatment of AMD.
- Establish the selectivity of the adsorbent with respect to particular metals.
- To characterize morphological transformation and chemical characteristics of the resultant solid residue.
- To examine the metal retention potential of banana peel in fixed-bed configurations of different flow rates and bed height conditions, using actual AMD.

1.4 Research Methodology

Batch studies were conducted to study the properties and to evaluate the adsorption capacity of the banana peel. Subsequently, column studies were also conducted to evaluate the performance of the banana peel adsorbent under continuous mode.

1.5 Dissertation layout

This dissertation consists of five chapters. Chapter 1 consists of the introduction, the problem statement as well as the aim and objectives of the study. In Chapter 2, the dissertation deals with a detailed literature review of the occurrence, chemistry and incidences of the AMD. It also gives the brief explanation of the current wastewater treatment techniques and brief explanation of adsorption phenomenon. This chapter also covers the explanation of different types of adsorbents and their properties. Chapter 3 comprises of a discussion of the material preparation and methodologies followed in this study. The methodologies include batch and column systems. The characterisation and results of the batch and the breakthrough curves for column adsorption of metal ions onto banana peel powder are discussed in Chapter 4. Conclusions drawn from the results are summarised in Chapter 5 of this dissertation.

CHAPTER 2

2. LITERATURE REVIEW

The mining of some minerals, including coal, copper, gold and manganese is linked with acid mine drainage problems that result in long-term impairment to watercourses and biodiversity (Akcil and Koldas, 2006). Acid mine drainage is a natural development that is being enhanced and intensified by mining activities (Johnson, 2003). It originates from mine waste rock, tailings, and mine structures, like pits and underground workings, and is mainly a function of the mineralogy of local rock material and the availability of oxygen and water (Valente and Gomez 2009). Rocks are exposed to weathering and discharge minerals as they come into equilibrium with their environment (Johnson, 2003).

Acid mine drainage is formed when sulfide bearing material or pyrite gets into contact with oxygen rich water (Akcil and Koldas, 2006). The pyrite undertakes oxidation in a two-stage process, initially generating sulfuric acid and ferrous sulfate and the additional orange-red ferric hydroxide and more sulfuric acid (McCarthy, 2011). Pyrite is part of an enormous amount of waste material produced through mining since minerals are commonly a rare addition to great amount of less value sediments (Mudd et al., 1999).

The weathering process of rocks and release of minerals is very slow in a natural environment. (Metesh et al., 1998). It is often accelerated by mining activities and it takes very short period of geological time, and also the mining activities pulverizes these rocks. This increases the surface area of the deposits that get into contact with water and the chances of water picking up the metals.

Consequently, the water gets acidic and poisonous to wild and plant life. The resultant acidic water dissolves heavy metals (iron, manganese, copper, zinc and others metals), and increase its toxicity. Some rock types comprise of minerals that can neutralize such acidity even when generated rapidly (especially calcium carbonate).

It can take up to 15 years for ferric iron to generate acid in a natural environment. However, the presence of bacteria speeds up the generation of this acid, and the regeneration time is reduced down to 8 minutes in existence of the bacteria, thiobacillus ferrooxidans (Metesh et

al., 1998). Due to the history of mining in South Africa, most of the deposits have been exhausted and mines closed (McCarthy and Humphrey, 2013). With the closure of mines numerous environmental problems have emerged. According to Experts team of inter-ministerial committee, the voids that are created by the termination of underground water extraction and hallows become flooded and overflow to the surrounding water catchments.

This occurrence was highlighted in September 2002, when the mine drainage began flowing from an abandoned shaft in the Mogale City/Randfontein area of the Western basin. As an outcome of the overflowing of the mines in this basin, a level of water began flowing out onto the surface. Nevertheless, the drainage programmes in the mining site may be the basis for main disruption in groundwater systems.

Mining activities may easily change the direction of the underground water movement, leading to interruptions in recharge and flow systems and drying up of certain streams. (Mudd and Ali, 1999). Although mining operations place environmental stress, it is, on the other hand, the source of major economic gains. It is very critical to efficiently manage the available water resources to the total mining activities and interrelated environmental impacts.

2.1 Gold mining

Witwatersrand mining begun as patchy open cast mining in the late 19th century and ended in the late 20th century leaving a complex network of channels, and extreme deep vertical chutes/sub-vertical shuts (Van Wyk et al., 2013). Gold was mined at the very deep end from the surface in Witwatersrand where an unoxidized pryritic ore was stumbled upon and rendered the process inefficient (Makgae, 2012), more than three ore bodies were mined to depths in excess of 3000 m. The cyanide extraction started around 1915 because it was highly selective for Au and Ag but it required finer milling (Van Wyk et al., 2013).

The resultant tailings from these mining activities were pumped to disposal sites, known as slimes dams and as a result mine dumps today are major contributors of acid mine drainage formation and heavy metal pollution. Representative heavy metals that have been identified and analysed from these dumps are As, Co, Cu, Pb, Mn and Zn (Tutu et al., 2008). Ground water and surface water in the region have been adversely affected by these conditions.

2.2 Coal Mining

One of the most abundant fossil fuel on earth is coal (Ramani, 2013). It forms part of about 75% of the total fuel resources (Elliot 1981). Witbank has a good quality coal but the mining activities worsen the surrounding environment including water, air and agricultural fields. The mixing of the coal and water increases the chemical constituents such as Ca, Mg, Fe, Cu, Zn and Mn, and has a negative impact on the farming soil (Harun-Or-Rashid et al., 2014).

Mining has triggered pollution of water, land sinking and air pollution. Mpumalanga has most of the abandoned coal mines (Bell et al., 2001). Coal mining can be done by opencast or underground mining method. In contrast of gold mining, the coal is removed from the mining area and the surface dumping is minimal. The host rock and the coal comprise of pyrite, but it is mainly in the coal layers.

Underground mining results in collapse of the top rock strata and when mining stops, the cavities in the cracked rock fill with water and decanting occurs from the deepest opening. The water reacts with pyrite in unmined coal in the host rocks and the water becomes acidic (McCarthy, 2011). This results in land sinking which leads to the surface cracking (Zhengfu et al., 2010), erosion of soil and air pollution, and decrease of biodiversity (Kibria et al., 2012). The well-being of society and agricultural economy is threatened by the contamination of the soil and water by heavy metals due to the coal mine drainage.

2.3 Chemistry of AMD

The most important mineral associated with acid mine drainage is iron disulfide (FeS_2). The variation of morphology such as particle size, crystallinity and reactivity affect the breakdown of pyrite, and crystals are less of an issue to weathering and oxidation than amorphic forms (Riley, 1960; Barnes and Romberger, 1968).
The exposure of pyrite to water and oxygen leads to it being oxidized and subsequent release of hydrogen ions, sulfate ions and soluble ions as shown in equation 2.1. The acidity of water is generally expressed as the logarithmic concentration of hydrogen ion in water or as pH.

$$2\,FeS_2\,(s) + 7O_{2(g)} + 2H_2O_{(l)} \rightarrow 2{Fe^{+2}}_{(aq)} + 4{SO_4}^{-2}{}_{(aq)} + 4{H^+}_{(aq)} \quad (2.1)$$

Further oxidation of Fe^{2+}(ferrous ion) to Fe^{3+} (ferric ion) follows when enough oxygen is dissolved in water or when water is exposed to the atmosphere (equation 2.2).

$$Fe^{2+}{}_{(aq)} + \frac{1}{2}O_{2(g)} + 2H^{+}{}_{(aq)} \rightarrow Fe^{3+}{}_{(aq)} + H_2O_{(l)} \quad ----------(2.2)$$

Ferric iron can either precipitate as a red-orange precipitate ($Fe(OH)_{3(s)}$) seen in water contaminated by acid mine drainage, or it can react directly with pyrite to produce more ferrous iron and acidity (Clark et al., 1997) as shown in equations 2.3 and 2.4.

$$2\,Fe^{3+}{}_{(aq)} + 6H_2O_{(l)} \rightarrow 2Fe(OH)_{3(s)} + 6H^{+}{}_{(aq)} \quad ----------(2.3)$$

$$14\,Fe^{3+}{}_{(aq)} + FeS_{2(s)} + 8H_2O_{(l)} \rightarrow 2\,SO_4^{2-}{}_{(aq)} + 15Fe^{2+}{}_{(aq)} + 16H^{+}{}_{(aq)} \quad ------(2.4)$$

From these reactions, it can be seen that under anaerobic conditions pyrite can remain in its reduced state as long as the strata is not disturbed. Though there are rare cases of naturally occurring acid channels, they mostly occur as a result of mining activities.

Iron sulfide that is situated beneath the water table in geological materials remains fundamentally stable, since the likelihood of oxidation is limited (Demchal et al., 2001). Nevertheless the sulfuric materials exposed to air become oxidizes and react, and water transports these reaction products into surface and groundwater. As the acidic water travels it continues to dissolve the other metals.

The degree of pyrite oxidation relies on numerous factors, including the concentration of oxygen, wetting and drying cycles, morphology of the sulphides, bacteria presence, acid consuming materials, and the geological history of the sulphides. Other sulfide minerals are associated with mineral deposits and some of these minerals produce sulfates and acidic medium, like the oxidation and hydrolysis of metal sulfides, chalcopyrite ($CuFeS_2$), sfalente (ZnS) and others release metals into solution in addition to sulphates and acidity.

As other sulfide minerals oxidise metalliferous drainage is formed, producing acidity although without producing (H^+). Acidity is thus present close to neutral pH water (Younger et al., 2002; Jennings et al., 2000).

2.4 Incidences of acid mine drainage in South Africa

Acid mine drainage(AMD) has affected a number of areas within South Africa, including the Mpumalanga and KwaZulu-Natal Coal Fields, Witwatersrand Gold Fields and the O'Kiep Copper District. Eastern, Western, and Central basins require immediate response after they have been identified as priority areas because of lack of sufficient measures to control and manage the problems related to AMD (Coetzee et al., 2010). Landscape around the mining towns have featured gold tailing dumps and has discharged polluted water for tens of years. Blesbokspruit has also been affected by the effects of this mined discharge (McCarthy, 2011). As reported by McCarthy and Humphries in 2013, the mining activities around the town of Caroline in Mpumalanga Province has polluted the Boesmanspruit dam which led to the contamination of water supply in the town. The closed mines are decanting extremely polluted water, and also the operational mines and coal handling facilities are added to the pollution of the water streams.

The polluted surface and groundwater of the severely affected lower Witrandspruit sub-catchment is entering these streams. The upstream of Witrandspruit is mainly a bedrock river and it widens on the lower sections where it feeds to a wetland. The sources of pollution seem to be located along the lower reach of the river.

Western basin in Gauteng has been flooded with acid mine drainage. The oxidation of pyrite contained in tailings dumps has contaminated and acidified the ground water in the mining district of Johannesburg and has elevated heavy metals concentrations (Naicker et al., 2003). The capillary rise and evaporation of the ground water have led to the severe contamination of the upper 20cm soil profiles by heavy metals. The contaminated ground water in the area contributes to approximately 20% of the stream flow and increase the acid content of the stream water.

The diversion of surface water away from mine dumps and working areas can prevent groundwater infiltration and hydrological seepage into impacted zones since the acid mine drainage follows the same pathways of water can be best managed by controlling water entry into these areas (Akcil and Koldas, 2006).

2.5 Treatment techniques

Control and minimisation continue to be the focus for best practice mine site management strategies, when AMD occurrence combine biological, chemical and physical approaches (Taylor et al., 2005).

2.5.1 Passive treatment

The passive treatment utilises natural processes to mitigate acid mine drainage - the contaminated water is diverted to a natural pond and wetlands for biological treatment that can achieve the same outcomes as the chemical treatments. These wetlands are categorised as aerobic, anaerobic and vertical flow. The aerobic wetland is mainly used for precipitation and aeration of metals from alkaline water while anaerobic wetland is used for acidic water (Kirby, 2014). This treatment method makes use of organic matter, plants and bacteria for treatment (Skousen and Ziemkiewicz, 2005).

2.5.2 Active Treatment

The most used technique to mitigate acid mine drainage is conventional active treatment processes (Bullen et al., 2003); including neutralisation, oxidation / reduction, extraction, sedimentation and flocculation, ion exchange as well as precipitation (Taylor et al., 2005). These processes vary in cost and effectiveness (Johnson and Hallberg, 2005), and have their short comings and limitations. The techniques based on ion exchange, chemical or biological oxidation have displayed low efficiency for trace contaminants removal (da Silveira et al., 2009). Sedimentation and flocculation as well as neutralisation techniques produce a bulky metal laden sludge that poses a disposal challenge.

Among available water treatment techniques, the adsorption process is regarded as a superior method because of its simplicity of design, ease of operation and convenience. It is a surface phenomenon which can also be defined in terms of unit operation in chemical engineering, and deals mainly with the application of surface forces and concentration of the materials on the body surfaces; referred to as adsorption (Bajpai and Rajpoot, 1998). In this process, applied in water treatment, ions are removed from the solution by adsorption onto solid surfaces (Worch,

2012). The adsorbed ions are called adsorbate and the adsorbing material is the adsorbent. At the active sites of the solid surface is where the adsorption occurs.

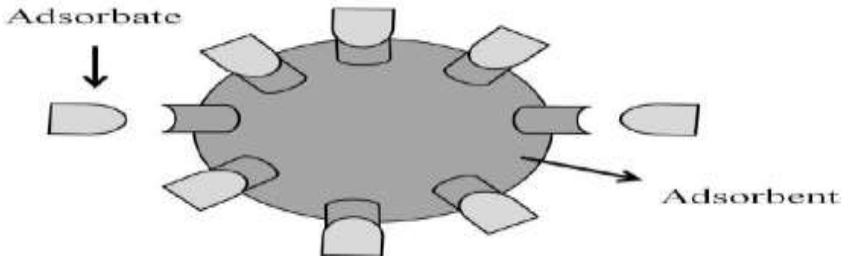

Figure 2.1. Mechanism of Adsorption (Neto et al., 2013)

The adsorption is a function of several factors such as pH, concentration of pollutants, contact time, particle size and temperature, and saturation is reached when the amount of the adsorbed species remain constant. The relationship between the amount of species adsorbed and the equilibrium concentration is called an isotherm (Ali, 2012).
Many different types of adsorbents have been developed. Some of the adsorbents used in removal of water pollutants are discussed herein.

Adsorption

Adsorption is a process through which ions from the solution adhere to the surface of solid material with which they are in contact. The ions are bound by chemical and/or physical interactions. The process creates a film of the adsorbed material on the surface of the adsorbing material (Babel and Kurniawam, 2003). There are two types of adsorption; namely, physical (physisorption) and chemical (chemisorption) adsorption.

Physical adsorption; is a process in which the adsorbate bonds to the adsorbent surface and micro pores by weak van der Waal forces. This phenomenon makes the physical adsorption reversible; bonds are easily formed and broken owing to the low adsorption energy that characterises the process.

Chemisorption is a result of chemical interaction between adsorbate molecules and adsorbent surface. This process is characterized by strong covalent or ionic bonds and high energy is

released. The process is irreversible as the bonds formed are strong and semi-permanent unless the adsorbate undergoes a chemical change (Somorjai, 1993).

The adsorption is affected by, but not limited to the following factors (Vasanth Kumar et al., 2004);

- Residence time - the longer the time the more enhanced is adsorption
- Particles sizes
- Surface area of adsorbent material - the smaller particle size implies a greater adsorption capacity
- Molecule size relative to pore adsorbent pore size
- Affinity of the solute for the adsorbent
- Solubility of the adsorbate - semi-soluble substances are more likely to adsorb than highly soluble substances.

Freundlich and Langmuir adsorption isotherms are the most largely used isotherms for the characterization of the adsorption phenomenon.

Freundlich isotherm model. This model describes the reversible adsorption and it is applicable to multilayer adsorption, with random distribution of adsorption heat and affinities over the heterogeneous surface. The total amount of the solute adsorbed is the sum of the adsorption on all sites with the stronger binding sites being occupied first, until the adsorption energy is exponentially decreased upon the completion of the adsorption process (Giwa et al., 2013).

The linearized Freundlich equation is given by:

$$log\ q_e = \frac{1}{n} log\ C_e + logK_f \quad ---------- \quad 2.5$$

Where $C_e,\ mg/l$ is the equilibrium concentration of the solute, q_e(mg/g) is the amount of metal adsorbed per unit mass of adsorbent at equilibrium, $K_f(mol/l)$ and n are equilibrium constants indicative of the adsorption capacity and adsorption intensity, respectively (Veli and Alyüz, 2007). n are values between 1 and 10 for this model indicate thermodynamically favourable adsorption (Falayi and Ntuli, 2014).

A plot of $log\ q_e$ vs $log\ C_e$ should be linear if the model fits the experimental data where:

$y = Bx + C, x = log\ C_e, y = logq_e, C = logK_f, B = 1/n$

Langmuir Isotherm model. The Langmuir isotherm assumes monolayer adsorption, with adsorption occurring at a finite number of definite localized sites that are identical and equivalent. It also assumes that there are no lateral interactions and steric hindrance between the adsorbed molecules, even on adjacent sites. It is characterized by homogeneous adsorption, where each molecule possesses constant enthalpies and sorption activation energy, with no transmigration of the adsorbate in the plane of the surface (Giwa et al., 2013)

It is characterized by an equilibrium saturation point where once a molecule occupies a site, no further adsorption can take place. Langmuir theory relates to rapid decrease of the intermolecular attractive forces with increase in distance (Jain et al., 2016).

The linearized Langmuir equation is given by;

$$\frac{1}{q_e} = \frac{1}{bq_m\, C_e} + \frac{1}{q_m} \quad \text{---------- 2.6}$$

Where C_e, mg/l is the equilibrium concentration of the solute, q_e(mg/g) is the amount of metal adsorbed per unit mass of adsorbent at equilibrium, q_m(mg/g) is the maximum adsorption capacity, b (L/g) is a constant related to enthalpy of adsorption. The amount adsorbed per unit mass of adsorbent at equilibrium q_e is given by:

$$q_e = (C_0 - C_e) \times \frac{V}{M} \quad \text{---------- 2.7}$$

Where C_0 (mg/l) is the initial metal concentration in solution, C_e (mg/l) is the equilibrium concentration in solution , V (L) is the volume of solution in litres and M (g) is mass of adsorbent in grams, A plot of $\frac{1}{q_e}$ vs $\frac{1}{C_e}$ should be linear if the model fits the experimental data where;

$y = Bx + C$, $y = \frac{1}{q_e}$, $B = \frac{1}{Kq_m}$ $C = \frac{1}{q_m}$, $x = \frac{1}{C_e}$

The Langmuir isotherm can be characterized by a dimensionless constant $R_L = \frac{1}{1+bC_o}$ called equilibrium constant (Juang et al., 1997). The R_L values indicate the type of isotherm where $0 < R_L < 1$ indicates that the adsorption is favourable (McKay et al., 1982).

Adsorption kinetic models. The Lagergren pseudo first order and pseudo second order models are some of the most commonly used adsorption kinetics models. A good correlation of the kinetic data explains mechanism of adsorption of the metal ion on the solid surface (Wu et al., 2001).

Pseudo first order kinetics

Pseudo first order kinetics is defined by the integrated equation:

$$\log(q_e - q_t) = \log q_e - \left({}^{k_1}/_{2.303}\right) t \quad \text{----------} \quad 2.8$$

Where q_t (mg/g) is the amount of metal ions adsorbed on the adsorbent at time t(min), q_e (mg/g) is the amount adsorbed at equilibrium, k_1(min^{-1}) is the rate constant of first order adsorption. A plot of $\log(q_e - q_t)$ vs t should be linear if the model fits the experimental data where

$y = Bx + C$, $y = \log(q_e - q_t)$, $B = {}^{k_1}/_{2.303}$, $C = \log q_e$

Pseudo second order kinetics

The pseudo second order kinetics is defined by the integrated equation below:

$$\frac{t}{q_t} = \frac{1}{k_2 q_e} + \frac{1}{q_e} t \quad \text{----------} \quad 2.9$$

where k_2 (kg/mol^{-1}.min^{-1}) is the rate constant of the second order model. A plot of $\frac{t}{q_t}$ vs t should be linear if the model fits the experimental data, and this will suggest that the rate limiting step may be chemical sorption involving valance forces through exchange of electrons between heavy metal ions and the adsorbent.

$y = Bx + C$, $y = \frac{t}{q_t}$, $B = \frac{1}{q_e}$, $C = \frac{1}{k_2 q_e}$.

Adsorbent material. An adsorbent is a solid material that attracts species from fluid phase onto its surface. Adsorbents are either of natural origin or the result of an industrial production and/or activation process. General natural adsorbents are clay minerals, natural zeolites, oxides, or biopolymers. Engineered adsorbents can be categorized into carbonaceous adsorbents, polymetric adsorbents, oxidic adsorbents, and zeolite molecular sieves, and these adsorbents are often very expensive. The adsorption capacity of natural and other low-cost adsorbents are much lower and the properties are subject to stronger variations (Lemley et al., 1995).

Agricultural waste. Cellulosic agricultural waste materials are adsorbents that are readily available in large quantities for significant adsorption of heavy metals. The functional groups in agricultural waste biomass include carbonyl, alcoholic, sulfhydryl, carboxyl, amino groups and others. These functional groups have affinity for heavy metal ions to form metal chelates. The mechanism of a biosorption process comprises adsorption on the surface, chemisorption, complexation, diffusion through pores and ion exchange (Sud et al., 2008)

Utilization of cheap natural agricultural waste that is in abundance for the removal of contaminants from aqueous solutions is very economical compared to other physicochemical processes (Marvrov, 2006). The plant waste is used as adsorbent worldwide for waste water treatment (Montanher et al., 2005). Banana is one of the most widespread fruits in the world and its benefits are not only edible but its peel has shown capability of removing heavy metals at significant capacity (Al-Azzawi et al., 2013).

*Activated Carbon.*Activated carbon is a black solid porous carbonaceous material. Its absence of impurities and oxidized surface distinguishes it from elemental carbon (Mattson and Mark, 1971). The general starting materials are coal, peat, lignite, charred wood and any organic material including animal bones, blood sewage sludge may be used with fair success (Buekens and Zyaykina, 2001).

Carbon source are activated and carbonized and most of the non-carbon elements are removed by pyrolytic decomposition of the source material. Organic material such as peat, sawdust, coconut shells, wood, and an initial carbonization process is necessary to transform the cellulose structures into carbonaceous material.

Figure 2.1. Activated carbon granules.

Zeolite. Zeolites, also known as molecular sieves, are crystalline silicates with a general chemical formula $Me_{2/n}O.Al_2O_3.xSiO_2.yH_2O$ (n = valence) containing oxides of alkali- or alkali-earth metals (Na, K, Ca) and characterised by regular structure of the pores with their dimensions in the range of the size of a molecule (Buekens and Zyaykina, 2001).

Different natural zeolites have shown changing ion-exchange capacity for cations like heavy metal ions. Other zeolites adsorbs organic and anions from aqueous solution. Natural zeolites can be modified numerous methods like surfactant functionalisation, ion exchange, acid treatment, making the zeolites to realize higher capacity for adsorption of organics and anions Natural zeolites are compact in size and they allow simple and cheap maintenance in the full-scale applications (Margeta et al., 2003).

Bentonite clay. Clays are hydrous aluminosilicates minerals that constitute the colloid segment of the soils, sediments, rocks, and water (Pinnaviaia, 1983) and may consist of blends of fine grained clay minerals and clay-sized crystals of other minerals such as carbonate, metal oxides and quarts (Srinivasan, 2011). Clays have various applications and properties that relies on their composition and mineral structure. The high specific surface area of clays and cation exchange capacity made the clay to have high adsorption capacity which may exceed that of activated carbon under same conditions of temperature and pH (Lin and Juang, 2002).

Montmorillonite mainly bentonite is the most promising for use in decontamination and disposal of heavy metals waste (Takahashi et al., 1987) on account of its higher surface area, cation exchange capacity and adsorption affinity for organic and inorganic ions. Bentonite is a

2:1 platelet mineral with one octahedral sheet between two silica sheets which forms layers (Mitchel et al., 1993).

Figure 2.2. Bentonite powder

2.6 Characterisation techniques

2.6.1 Scanning electron microscope

The scanning electron microscope (SEM) uses a focused beam of high-energy electrons to generate a variety of signals at the surface of solid specimens (Swapp, 2016). The electrons interact with the sample atoms producing signals that contain information about the sample's surface topography, composition and other properties such as electrical conductivity. In many applications, the data is collected over a selected area of the sample surface and a two-dimensional image is generated that displays spatial variations in these properties (Liu et al., 2010).

Signals produced by an SEM result from interactions of the electron beam with atoms at or near the surface of the sample, include secondary electrons, back-scattered electrons (BSE), characteristic X-rays, light (cathodoluminescence), specimen current and transmitted electrons. By detection of secondary electron, SEM can produce vivid images of a sample surface (secondary electron image, or SEI), with superior resolution about 1 to 5 nm. Characteristic X-rays are emitted as the electron beam removes an inner shell electron from the sample, causing a higher energy electron to fill the shell and release energy. These X-rays can be used to identify and quantify the elements in samples. SEM analysis is considered to be non-destructive, that is, x-rays generated by electron interactions do not lead to volume loss of the sample, so it is possible to analyse the same materials repeatedly (Reed, 2005).

2.6.1 Fourier-Transform infrared

Fourier-Transform infrared (FTIR) spectroscopy is a vibrational spectroscopy that records absorptions of Infra-Red (IR) light by chemical bonds in all molecules. Since different bonds absorb IR light at characteristic but different wavelength FTIR spectroscopy is often referred to as fingerprint spectroscopy. As a consequence pure compounds have characteristic and unique FTIR spectra when infrared radiation is passed through a sample. The sample analysis process entails the emission of infrared radiation from a black body source. The beam of radiation passes through an aperture which controls the amount of energy presented to the sample and ultimately to the detector. The beam enters the interferometer where the spectral encoding takes place. The resulting interferogrm signal exits the interferometer. Therefore FTIR can identify unknown materials, the quality of a sample and components of a sample (Griffiths and De Haseth, 2007)

CHAPTER 3

3. MATERIALS AND METHODS

This chapter describes in details the materials and methodologies including the research instruments, the data and analysis used in the determination of banana peels as potential adsorbent for AMD treatment. The characterization of the banana and preparation of banana peels and analysis of different solutions used in this work is also discussed.

3.1 Materials

3.1.1 Material preparation

Banana peels were collected from local supermarkets. The pith on the peel was removed and the peels were cut into small pieces (1-2cm), then washed with deionised water to remove external dirt and dried in an oven at 80°C for 24 hours. The peels were crushed to reduce particle sizes then soaked into deionized water for 6 hours to remove the yellow pigment and dried again for 6 hours at 80°C.

3.1.2 Chemicals

All the chemicals used in this work were of analytical grade and actual AMD was collected in four 25L bottles from Kromdraai decant. The synthetic single component stock solutions of 1 g/L of Mn, Zn and Cu were prepared by separately dissolving 3.17g, 4.4g and 3.93g of analytical grade of $MnSO_4.4H_2O$, $ZnSO_4.7H_2O$ and $CuSO_4.5H_2O$, respectively. The desired concentrations were prepared by successive dilutions of the stock solutions.

3.1.3 Synthetic single component, ternary component solution and actual acid mine drainage

The stock of synthetic water with single component with concentration of 50 mg/L of Mn, Cu and Zn were prepared by adding predetermined quantity of analytical grade of $MnSO_4.4H_2O$, $CuSO_4.5H_2O$ and $ZnSO_4.7H_2O$ into deionized water as per investigated parameters. The pH

was adjusted to 3.0 ± 0.2 by using 0.2N sulphuric acid and 0.1N sodium hydroxide. Ternary synthetic solution comprised of the mixture of Mn, Cu and Zn at equal concentration.

The AMD used to investigate the potential of banana peels in removing heavy metals was collected in four 25L drums from Kroomdraai decant. One drum was fortified with $ZnSO_4.7H_2O$ and $CuSO_4.5H_2O$ to increase the concentration of Zn and Cu metals respectively, for comparison.

3.1.4 Surface area and porosity

The specific surface area of the banana peel powder used in this study was calculated using the Brunauer-Emmett-Teller (BET) equation, and the results of analyses were reported before and after the adsorption of the metals in the AMD.

3.1.5 Surface morphology and functional group of the banana peels

The banana peels used in this study were left at natural state with no chemical or thermal treatment. The banana peels were washed and soaked with distilled water to remove dust, pigment and other external dirt on their surfaces before use. The surface morphology and functional groups of the banana peels were studied before and after adsorption by scanning electron microscope (SEM) and Fourier-Transform infrared (FTIR) spectroscopy respectively.

3.2 Experimental methods

3.2.1 Batch adsorption studies

Batch adsorption studies were carried out using banana peels mixed with solutions containing the desired concentration of heavy metal ions. The mixtures of 200mL were agitated in 250 mL plastic bottles in a shakerbath at 200 rpm. The value of the agitation rate was chosen arbitrarily since there are many variables that affect agitation and is very difficult to duplicate all of them at larger scale.

Adsorbent particle size distribution

The crusher (Ika Werke M20) and vibrating sieves were used for the reduction of particle size of the dried banana peel and for particle size distribution, respectively. The sieves were mechanically vibrated for 15 minutes which was sufficient for separation to take place. The screens were subjected to weighing balance before and after the vibration to get the mass and size of the banana peel particles retained on each sieve. The particle size range of 0.15 mm to 5 mm was carefully chosen with the intention to investigate how adsorption changes with the change in particle size and to reduce problems associated with filtration of adsorbent in batch systems and pressure drop in an adsorption column systems.

The effects of adsorbent particle size on percent removal of heavy metals were investigated. Four different sieve aperture sizes were used $d_s<0.15$, $0.15\leq d_s\leq 0.4$, $0.4 \leq d_s \leq 1$, and $1\leq d_s \leq 5$ mm (d_s = sieve arpeture diameter in mm) to distribute 3.2 kg of banana peel. About 1000 mg of adsorbent at the required particle size was mixed with 200 mL solution of the appropriate single component solution. The contact time to saturation of plants based adsorbent is generally less than 90 min (Jain et al., 2016; Kanyal and Bhatt, 2015; Deshmukh et al., 2017), to avoid ambiguity the contact time of 180 minutes was chosen for the study. Furthermore, to keep energy costs low, the experiments were carried out at room temperature (22°C). Samples were collected at regular time intervals (5, 10, 20, 30, 45, 60, 180 minutes) and analysed using an ICAP Q Inductively-Coupled Plasma Mass Spectrometer (ICP MS).

Effect of adsorbent mass

Six different masses of banana peels (i.e., 200, 400, 600, 800, 1000 and 1200 mg) were used in 200 mL aqueous solution. The mixture was agitated for 180 minutes and samples for analysis were taken at regular intervals (5, 10, 20, 30, 45, 60, 180 minutes). The particle size of.$15 \leq d_p \leq 0.4$ mm was chosen to avoid pressure drops in column systems.

Kinetic Studies

The banana peels of 1000 mg in 200mL solution was used to study the effects of contact time for single component solution, fortified and actual AMD at room temperature(22°C). The contact time was 180 minutes and each samples was collected in the following time intervals: 5, 10, 20, 30, 45, 60, 180 minutes.

Effect of initial solution pH

The solution pH was varied as follows: 2.0, 3.0 and 5.0±0.2 in order to avoid the precipitation of heavy metals above the pH of 5 (Wu et al., 2012). Solution pH was adjusted using 0.2 N H_2SO_4 and 0.1N NaOH. The solution was agitated for 180 minutes at room temperature (22°C). The final pH of the solution was also measured.

Effects of initial solution concentration

The effect of initial metal concentration on the removal of the heavy metals from solution by banana peels was investigated by contacting 1000 mg of banana peel powder in a 200 mL of a single component solution with concentration ranging from 25 mg/L to 100 mg/L. The experiments were run for 180 minutes.

Selectivity of the adsorbent

The AMD generally comprises of more than one cation, i.e., it is a mixture of different heavy metals such as Ni^{2+}, Cd^{2+}, Fe^{3+}, Pb^{2+}, Cu^{2+}, Cr^{3+}, $Mn^{2+,}$ Zn^{2+}, etc. Tests were performed to investigate the influence of the presence of other cations on the adsorption capacity of banana peels for heavy metals under investigation in this study. Solution containing equal concentrations (ternary component solution) of Mn^{2+}, Zn^{2+} and Cu^{2+} was agitated with banana peel at room temperature (22°C) for 180 minutes. About 50mg/L initial concentration of three components solutions (i.e Mn, Zn and Cu metal ions) were prepared at a pH of 3±0.2 to mimic the pH of the actual AMD collected from Kromdraai decant. Furthermore, the investigation

was also conducted on actual AMD and fortified AMD. The actual AMD collected for the study had no Cu metal ion and had low concentration of Zn metal ion, hence the AMD was fortified.

Equilibrium adsorption isotherms

Equilibrium adsorption isotherm experiments were conducted by contacting different adsorbent loading of 200, 400, 600, 800, 1000 and 1200 mg with constant fixed initial concentration of the metals in a fixed volume (200 mL) of solution at room temperature (22°C). The mixture was agitated in a shakerbath for 180 minutes. Thereafter, samples were taken filtered and analysed using an ICP MS.

3.3 Column studies

Fixed bed column experiments were carried out in a laboratory scale perspex columns with a fixed diameter of 3.5 cm and height of 50 cm as shown in Figure 3.1 below. The column was fitted with a polymer beads and glass wool at both ends to keep the adsorbent bed in fixed position.

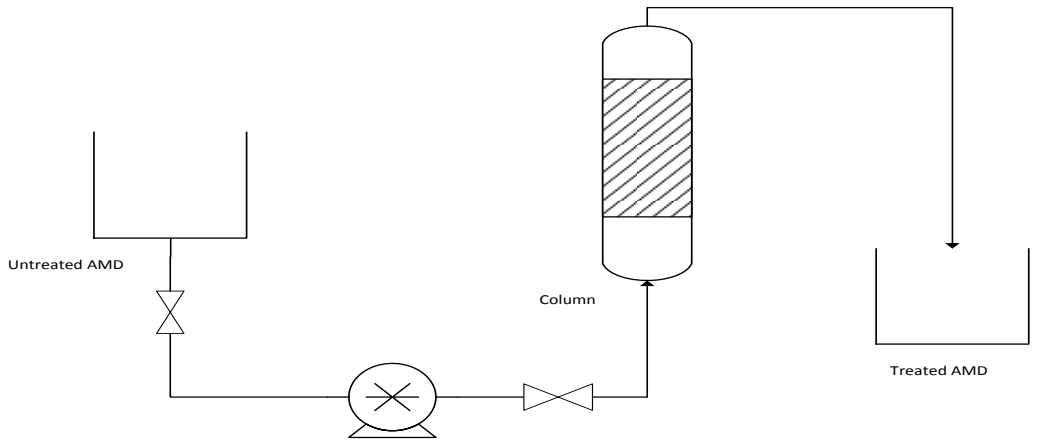

Figure 3.1 Schematic diagram depicting the setup for the adsorption column

An AMD sample for the study was collected from Kromdraai decant in Witbank. The experiments were carried out to study the effects of bed depth and flowrate of the influent on the adsorption of Mn and Zn. The concentrations of Mn and Zn in actual AMD solution was 46.006 and 3.505 mg/L respectively, at the pH of 3.12. The flow rate and the bed depth were arbitrarily chosen since there is no literature information relating to this experiment. The bed depth range investigated was 6 to 17.8 cm at the fixed flowrate of 15 mL/min while the flowrate investigated ranged from 15 to 45 mL/min at the fixed bed depth of 17.8 cm. The column was fed from the bottom so as to reduce gravity assisted channelling and the samples of the treated actual AMD solution were collected from the top of the column at different time intervals and analysed using ICP MS. The samples were collected and analysed until bed saturation was reached.

3.4 Data analysis

The experiments were carried out in duplicate and the mean values were reported.

CHAPTER 4

4. RESULTS AND DISCUSSION

4.1 Batch studies

4.1.1 Particle size distribution

The size distribution of the banana peel particle is shown in figure 4.1. The banana peel particles were distributed on the mechanically vibrated sieve. The particle size range of $0.15<dp<0.4$ mm was practically chosen with consideration of the potential for scalability where filtration challenges and pressure drop can be reduced and the effects of the changes in particle size on adsorption of heavy metals is discussed in section 4.1.8.

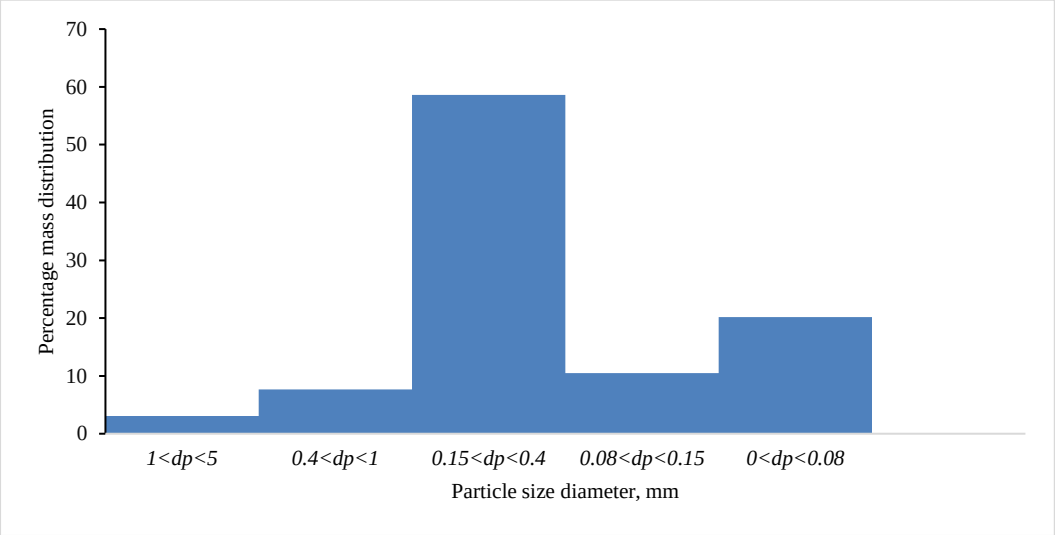

Figure 4.1 Particle size distribution of the banana peel.

4.1.2 Surface area and porosity

The specific surface area of the banana peel adsorbent at different particle size listed in Table 4.1 was less than 1 m^2/g. This range of surface area is in agreement with other studies on fruit peels (Chao et al., 2014). The surface area of the particle size chosen for the study was 0.011 m^2/g.

Table 4.1 Surface area of the banana peel particle size

Adsorbent	**Particle size(mm)**	**BET surface area (m^2/g)(x 10^{-5})**
Banana peel	5	1.813
	1	6.010
	0.4	1135
	0.15	1214

4.1.3 Surface morphology and functional group of the banana peel powder.

Scanning electron microscopy (SEM) was used as a tool for studying surface morphology and fundamental physical properties of the banana peel. The characterization of the banana peel powder before (Fig 4.2a) and after (Fig 4.2b) adsorption showed a change in the surface morphology of the adsorbent. Rough surface texture and porosity could be distinctly noticed after adsorption. Spent banana peel (Fig 4.2b) shows a less compacted surface of the banana peel than the original (Fig 4.2a) compacted surface, furthermore, peels have a surface partially covered by heavy metals after the adsorption.

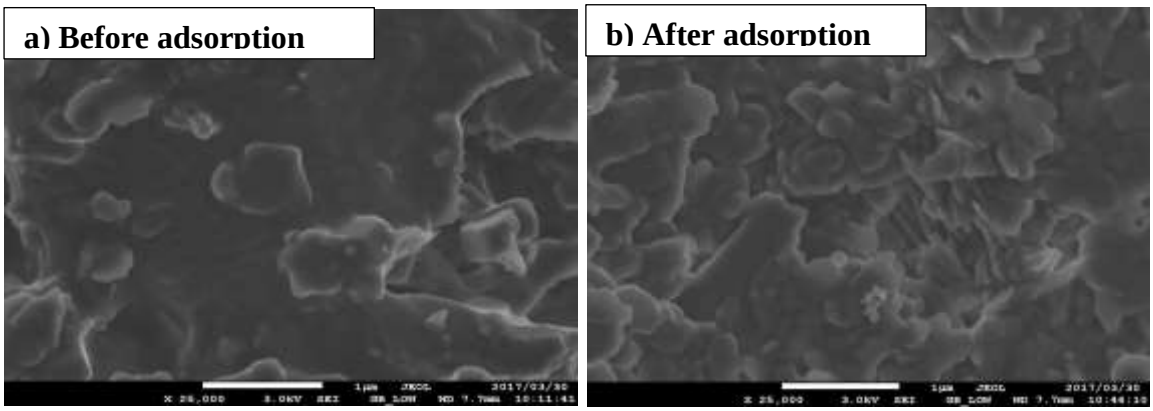

Figure 4.2 Scanning electron microscopy of banana peel before (a) and after (b) adsorption of heavy metals.

The FT-IR spectra shown in figure. 4.3a and 4.3b were obtained in order to understand the nature of the functional groups in the banana peel. The FTIR spectra in Figure 4.3a and 4.3b shows a number of peaks, indicating the nature of the banana peel adsorbent. The peaks observed at 2920 cm^{-1} can be attributed to the C-H stretching alkane groups. Bands appearing at 1706, 1734, 1290, 1212, 1246, 1614,2852, 3020, and 3386 cm^{-1} in Figure 4.3a and figure

4.3b were assigned to stretching carboxylic acid dimer, COO^- anion stretching, C-O stretching aromatic ester, stretching secondary alcohol, C-O stretching alky aryl ether, N-H stretching amine salt, O-H stretching alcohol, and N-H stretching aliphatic primary amine respectively. Hydroxyl and carboxylic acid played a key role in the removal of divalent metals, Zn, Cu and Mn. The peak observed at 1412 cm^{-1}in Figure 4.3b is attributed to nitrates. It indicates that the banana peel has adsorbed the nitrates from the AMD. The adsorption of the metals did not change the position of the peaks. The intensity of the peaks for functional groups of the adsorbent has been reduced this may be due to the coverage of the surface of the banana peel by the adsorbed ions.

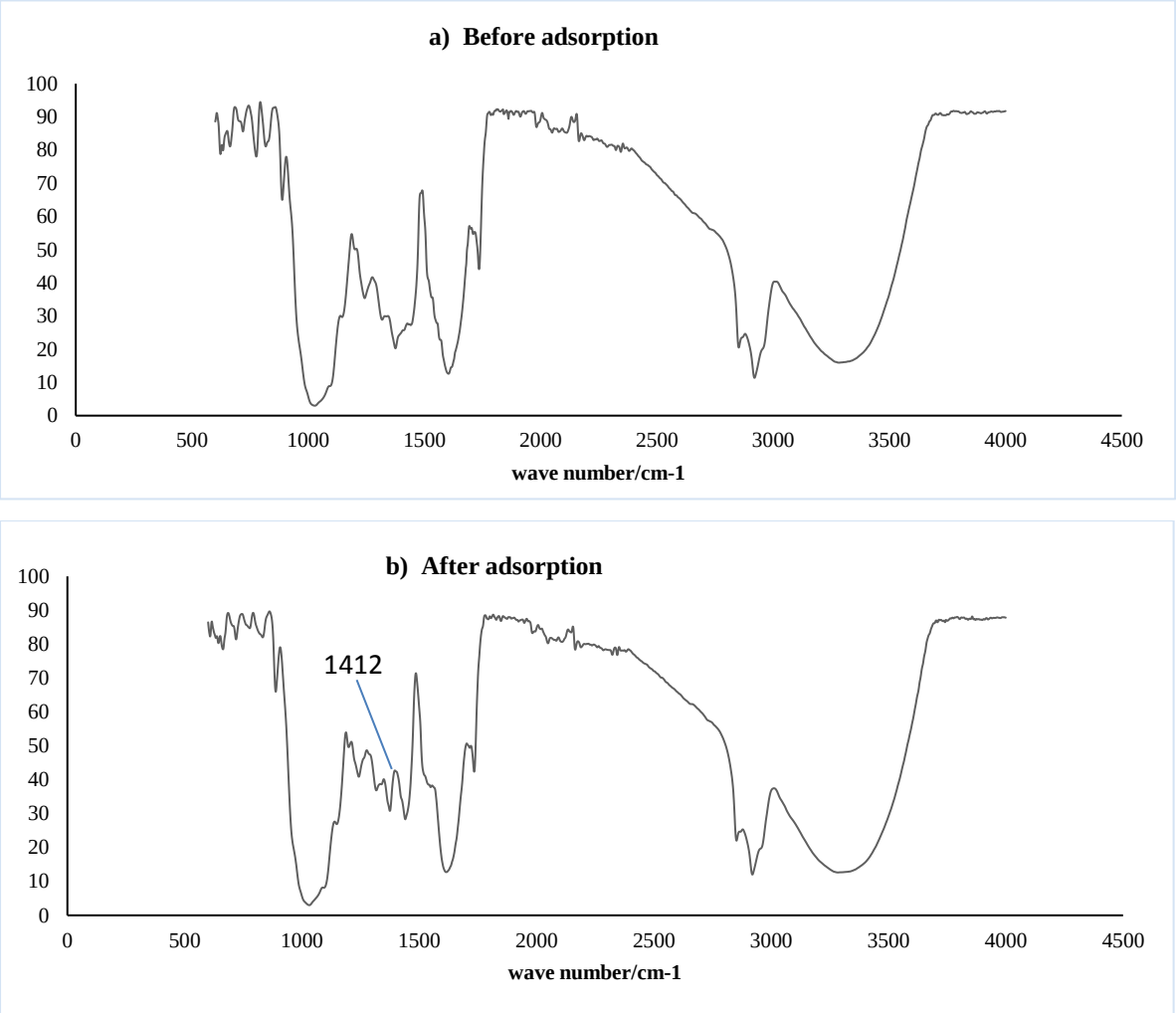

Figure 4.3 The FTIR spectra of the banana peel powder before and after adsorption.

4.1.4 Effect of adsorbent dosage

A series of kinetic experiments at different adsorbent mass, that is, 200 mg, 400 mg, 600 mg, 800 mg, 1000 mg and 1200 mg were conducted using a fixed initial concentration for the respective metal. Typical plots of the amount of metal adsorbed as percentage removal are shown in Figure 4.4a, 4.4b and 4.4c.

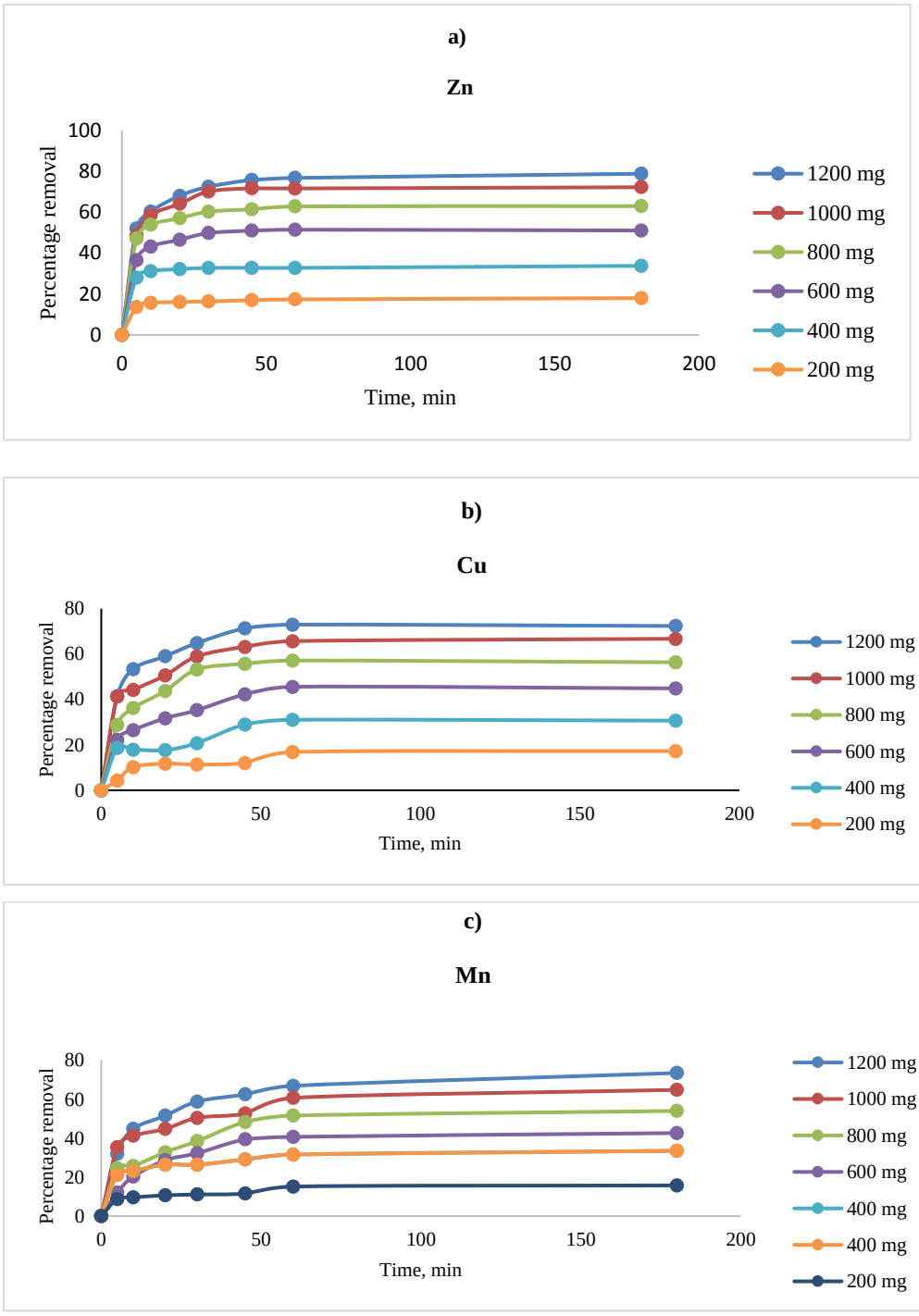

Figure 4.4 The effects of the mass dosage of banana peel powder on the adsorption

These figures indicate that the sorption was quick, and the saturation was reached at about 45 minutes for Zn and Cu. The results show that Zn, Cu and Mn percentage removal increase with the increase in adsorbent dosage. Furthermore, the Zn removal percentage is higher than Cu of which is higher than Mn at all dosage investigated. In order to circumvent the error in the experiments, sorption time of 180 min was adopted for subsequent studies. The increase in percentage removal with adsorbent dosage can be attributed to an increase in adsorption sites per unit mass of adsorbent.

4.1.5 Effects of initial concentration

Figure 4.5 shows that percentage adsorption of Zn, Cu, and Mn decreased with increasing initial concentration. For example, at the initial concentration above 50 mg/L (i.e 80 mg/L, 100 mg/L), Zn decreased from 72.43% to 67.75%, Cu decreased from 64.10% to 61.57% and Mn decreased from 62.61% to 43.14 %. However, the amount of metal ions adsorbed per unit mass of banana peel increased with an increase in initial metal ion concentration this is in concordance with Iqbal and Edyvean, 2004. This increase could be due to an increase in electrostatic interactions relative to covalent interactions, involving sites of progressively lower affinity for metal ions (Al-Asheh and Duvnjak, 1995). The results also show that adsorption percentage with respect to Zn, Cu and Mn has reached a saturation point at 50 mg/l with the optimum percentage removal of 72.43%, 66.97% and 62.61% respectively.

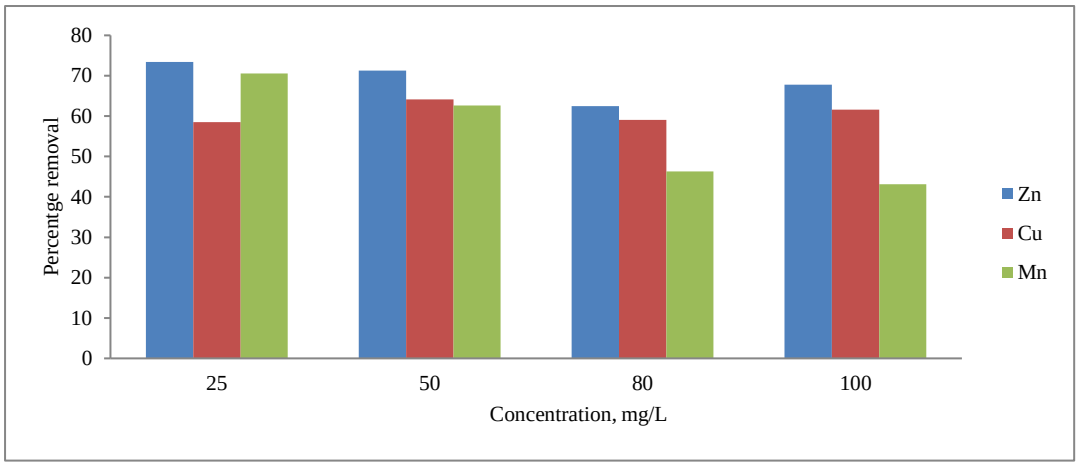

Figure 4.5 Effects of initial concentration on the adsorption of zinc, copper and manganese.

At all concentration level the banana peel has adsorbed more of Zn than Cu and more of Cu than Mn (Zn>Cu>Mn) at saturated point. This may be attributed to lower hydrolysis constant of Zn (7.53) and Cu(9.00) compared to Mn (10.70). The least values of hydrolysis constant contribute to low affinity of heavy metals to hydroxyl ions (Grzybkowski, 2006 and Moreno, et al., 2010) hence they adhere to the surface of the banana peel.

4.1.6 Equilibrium adsorption isotherms

The fitting of Langmuir and Freundlich models to experimental data for the adsorption of Zn, Cu and Mn are shown graphically in Figure 4.6*a* and Figure 4.6*b*. Figure 4.6*a* shows that Langmuir isotherm for the adsorption of Zn, Cu and Mn from solution gave good fit of the experimental results, as shown by the values of the correlation coefficient, R^2, which are 0.978, 0.950 and 0.971, respectively.

The linear plot of Freundlich equation for Zn, Cu and Mn adsorption are shown in Figure 4.6*b* and the calculated parameters are listed in Tables 4.2*a* and 4.2*b*. The Freundlich isotherm model was also best fitted with experimental data as it shows good correlation coefficient values of 0.932, 0.951 and 0.951 for Zn, Cu and Mn, respectively.

Adsorption of Zn, Cu and Mn all fit Langmuir and Freundlich very well and is in agreement with Anwar et al(2014) where these models both had a good fit to the data. However, these correlation coefficients are only limited to the degree of freedom of 5 that is arbitrarily chosen for this study. According to Langmuir model the adsorption capacity of the banana peel powder and model fit as listed in Table 4.2a was in this order, Zn >Cu>Mn. This order of adsorption capacity is in concordance with Wu et al 2014. The high adsorption of Zn may be attributed to its low hydrolysis (7.53) constant compared to Cu (9.0) and Mn (10.0). Since the values of $R_{L,}$ and n for all the metal ions ranges between 0 and 1, and 1 and 10 respectively, this indicates that the adsorption of these metals by banana peel is spontaneous (Falayi and Ntuli, 2014).

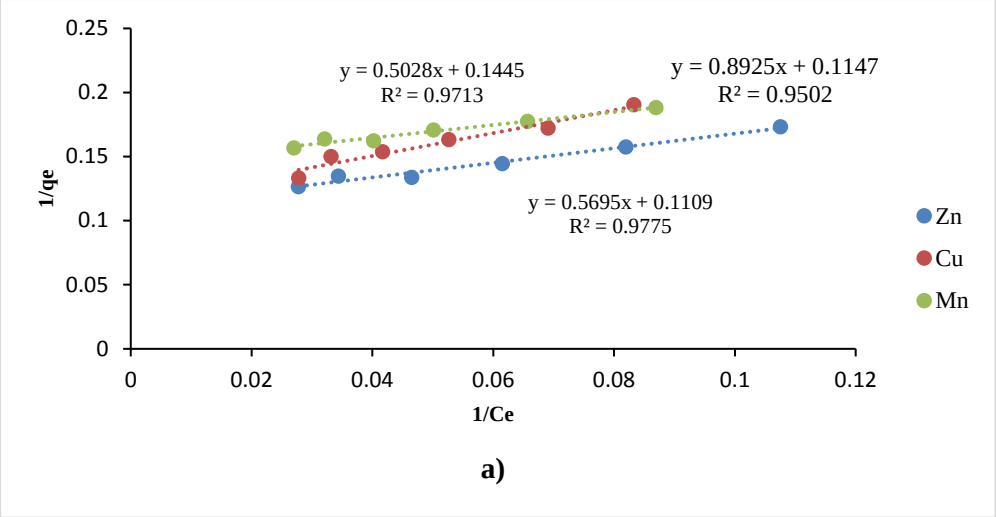

a)

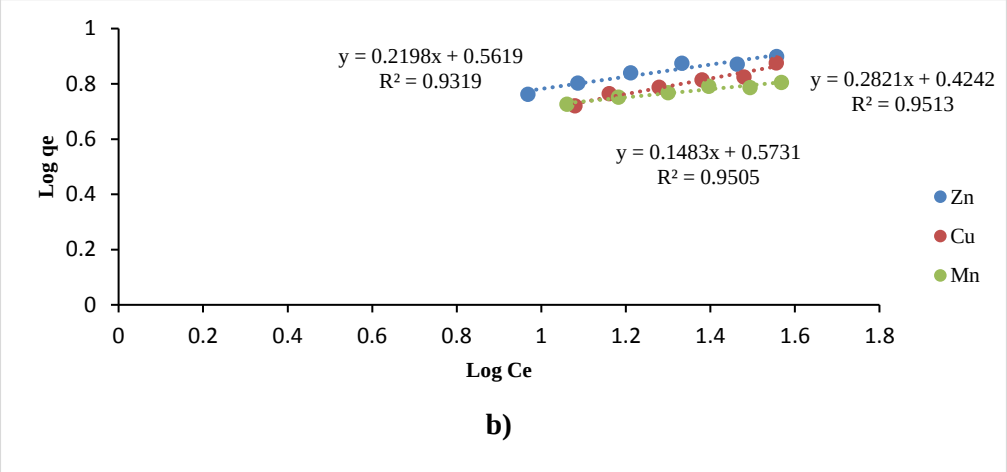

b)

Figure 4.6 Langmuir (a) and Freundlich (b) linear plot for sorption of metal ions

Table 4.2 Langmuir isotherm parameters and Freundlich isotherm parameters

a)

Langmuir isotherm parameters	**Zn**	**Cu**	**Mn**
$q_{m(mg/g)}$	9.017	8.718	6.920
b	0.195	0.129	0.287
R^2	0.978	0.950	0.971
R_L	0.105	0.151	0.080

b)

Freundlich isotherm parameters	Zn	Cu	Mn
K_f	3.647	2.656	3.742
n	4.550	3.550	6.743
R^2	0.932	0.951	0..951

4.1.7 Effects of solution initial pH

The pH of the solution in contact with the banana peel powder has an impact on its ability to remove metal ions. This is because the acidic solution has an influence on both the functional of the banana peel powder and exchange ions. The dependence of the heavy metal adsorption on pH is related to the surface functional groups in the banana peel powder. As stated in subsection 3.2.1.5 the experiments were conducted by varying the solution pH as follows: 2.0, 3.0 and 5.0±0.2 for the single component solutions whilst keeping all the other parameters unchanged.

Figure 4.7*a* below shows that the heavy metal removal efficiency improves with the increase in the pH of the single component solution, this is in agreement with similar study conducted by Wu et al., 2012 and Zhang et al., 2014. The removal efficiency of Zn, Cu and Mn at the pH range of 2.0 to 5.0 increased from 28.24% to 80.90%, 34.64% to 75.21% and 28.24% to 71.78 %, respectively. Furthermore, percentage removal of Zn is greater than Cu which is also greater than Mn. Low pH is inhibiting the adsorption of heavy metals onto banana peel powder, the heavy metals may be competing with H^+ ions for binding with the banana peel powder surface functional groups (Ingezakis et al., 2001). The Zn, Cu and Mn start precipitating at pH above 5 (Wu et al., 2012), hence the maximum pH studied for adsorption of these heavy metals was 5.

Figure 4.7*b* shows that the pH of the solution increases during the reaction, which may be attributed to the buffering effect of the banana peel powder because of its alkalinity.

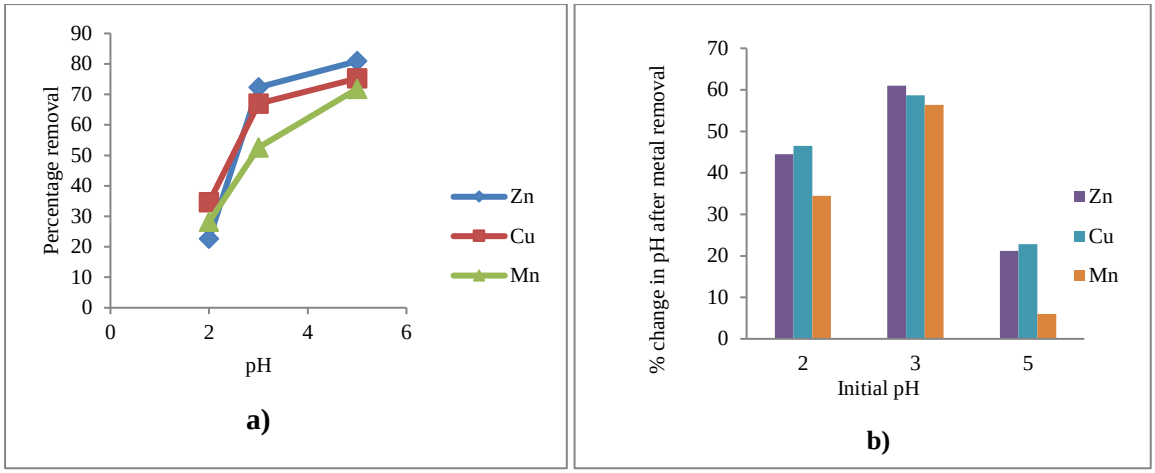

Figure 4.7 Effect of Initial pH on the percentage removal and Change in pH of the solution

4.1.8 Effects of particle size

Figure 4.8 shows that an increase in particle size results in lower heavy metal removal efficiencies. This is in agreement with the work of Giwa et al 2013 conducted on the husk of melon seeds. The removal efficiency is higher at the particle size of 0.15 mm, 74.56 %, 78.91% and 72.43 % for Zn, Cu and Mn, respectively and lowest at the banana peel powder particle size of 5 mm, 16.29 %, 15.71 % and 6.63 % for Zn, Cu, and Mn, respectively. The removal of Zn metal ions is higher than Cu and Zn except on 0.15 mm particles and this can be attributed to its low hydrolysis constant, in such that most of Zn metal ions in the solution do not form $Zn(OH)_2$. Therefore, from the results it can be seen that smaller particles size are more efficient in heavy metals removal. This is because smaller particles has a large area per Volume/Mass ratio for adsorption than larger particles. However, particles sizes that are less than 0.15 mm may cause difficulty in solid-liquid separation in batch mode, and significant pressure drops in fixed bed columns (Ingezakis et al., 2001)

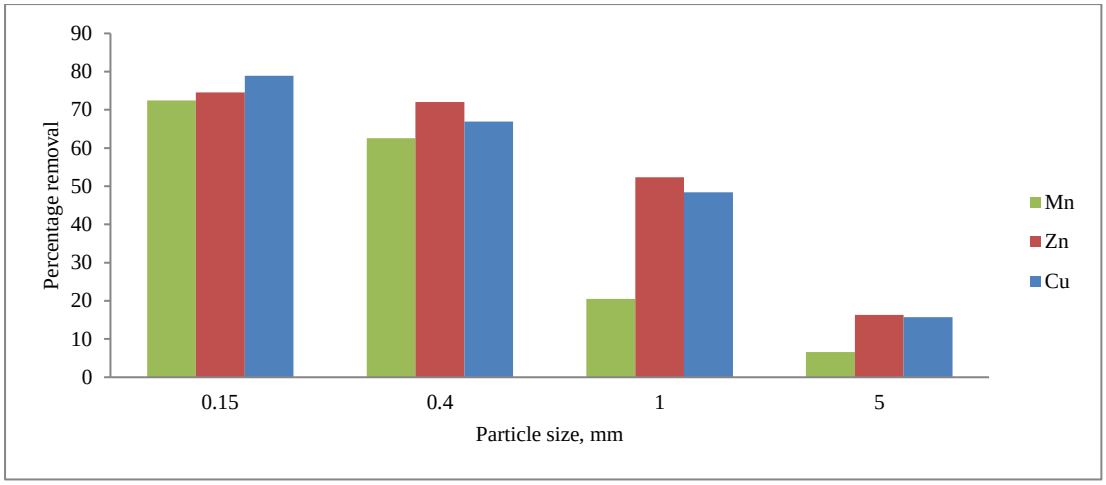

Figure 4-8 Effects of particle size on the adsorption of zinc, copper and manganese.

4.1.9 Effects of competing cations

The adsorption of Zn, Cu and Mn was significantly affected by competing cations as shown in Figure 4.9. The amount of the metal ion concentration removed was high for each metal ion in the single component solutions, 72.43, 66.97, and 62.61% for Zn, Cu and Mn metal ions respectively, the metal ion in each solution had no competition for the adsorption site of the adsorbent. However, after the metal ions were mixed to form a solution of ternary components solution 50.99, 54.96 and 35.07% for Zn, Cu and Mn metal ions, respectively in a constant mass of adsorbent, the removal efficiency of each metal ion decreased, and the three ions had to compete for the active adsorption site of the adsorbent. The banana peels removed more of Zn than Cu and Mn, this can be attributed to its low hydrolysis constant.

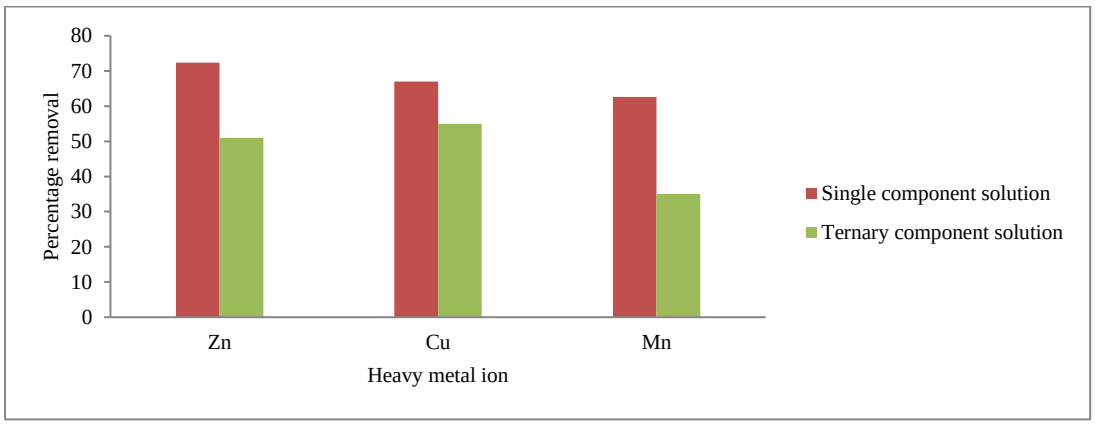

Figure 4.9 Selectivity of the banana peel powder.

4.1.9 Lagergren pseudo first order and second order plots

Table 4.3 and Figure 4.10 show that correlation coefficient values (R^2) are very low for all metals under the investigation, the experimental q_e values does not agree with calculated ones, obtained values from the linear plot. This further suggests that the adsorption of Zn, Cu, and Mn ions does not follow pseudo first order kinetics.

Table 4.3 Kinetic parameters for the adsorption of Zn, Cu and Mn on the banana peel peel powder.

Heavy metal ions	**Pseudo-first-order**					**Pseudo-second-order**			
	q_e experimental, mg/g	R^2	k_1(min^{-1})	q_e calculated, mg/g	Error %	R^2	k_2 (g/mg^{-1}.min^{-1})	q_e calculated, mg/g	Error %
Zn	6.345	0.878	0.074	2.492	60.724	0.9998	0.505	6.431	1.356
Cu	5.806	0.842	0.048	2.324	59.972	0.9994	0.215	5.974	2.894
Mn	5.634	0.577	0.022	2.110	62.548	0.9978	0.121	5.858	3.976

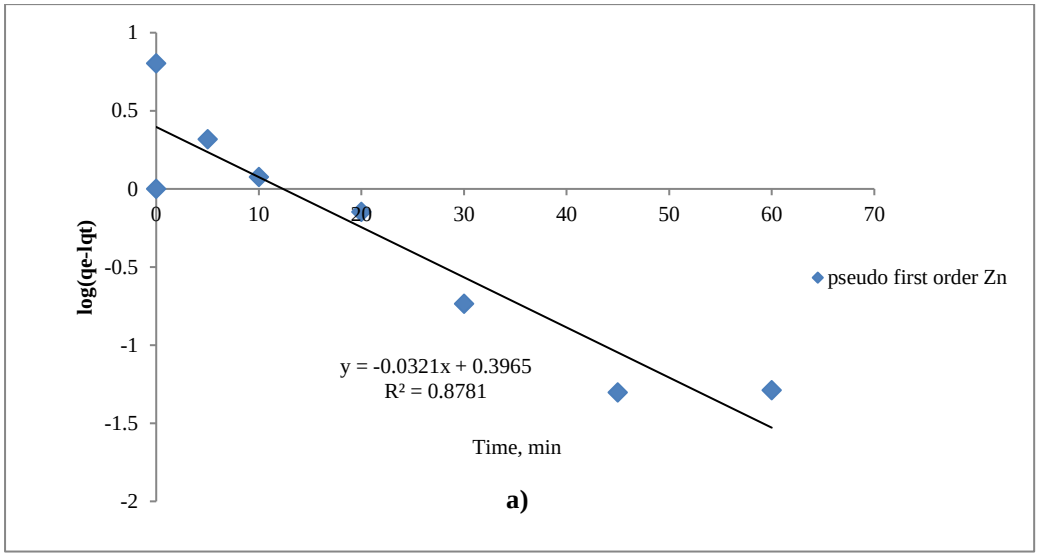

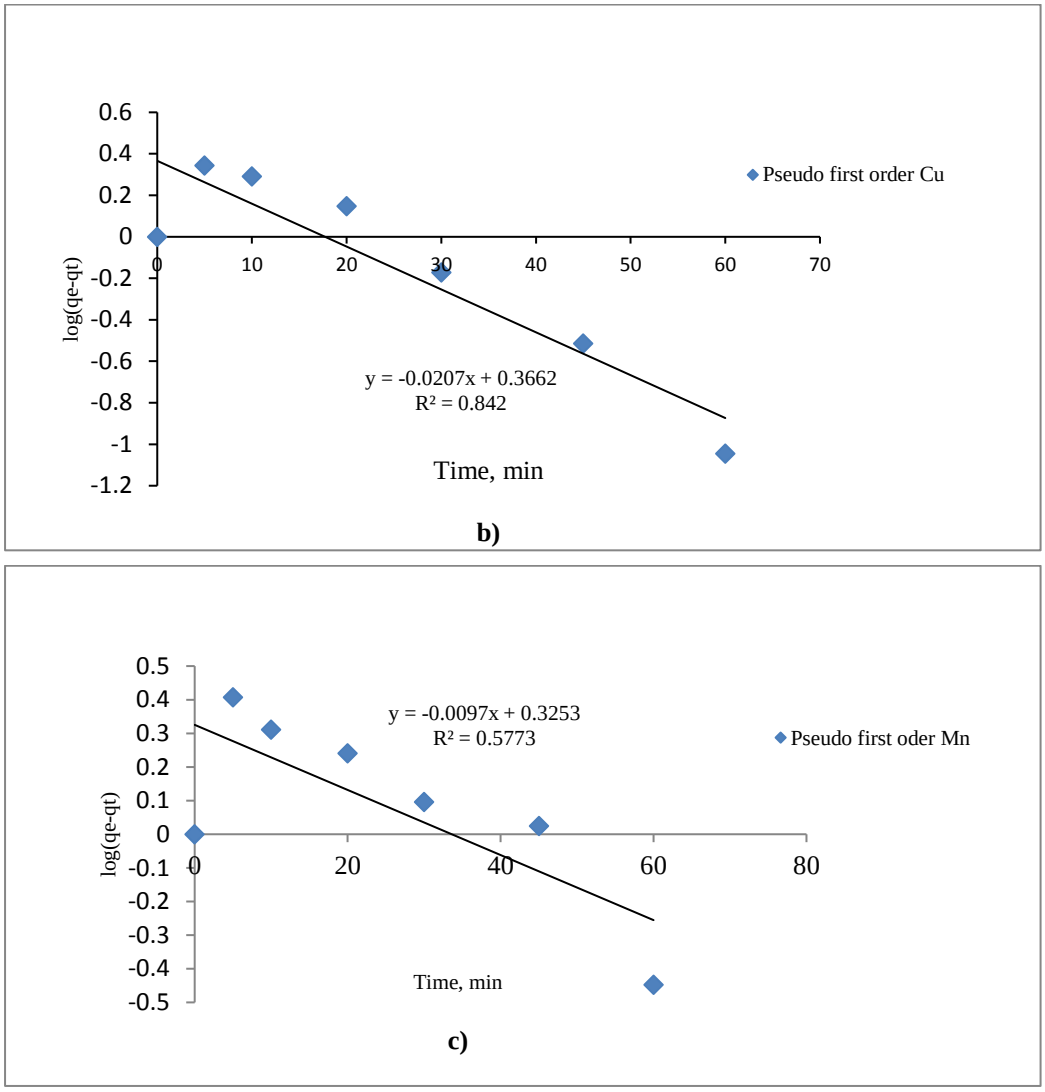

Figure 4.10 Pseudo first order plot for the adsorption metal ions.

The pseudo-second order rate constant k_2 and q_e values were calculated from the slope and intercept of the plots *t/q vs t* as shown in Figure 4.11. As can be seen from Table 4.3, the experimental values of q_e agree well with calculated *q*e values and the error is less than 5% for all the metals under investigation. This suggests that the rate-limiting step is chemical sorption that involves valance forces through exchange of electrons between banana peel powder and heavy metals ions, thus the adsorbent exhibited high performance in the adsorption divalent heavy metal ions.

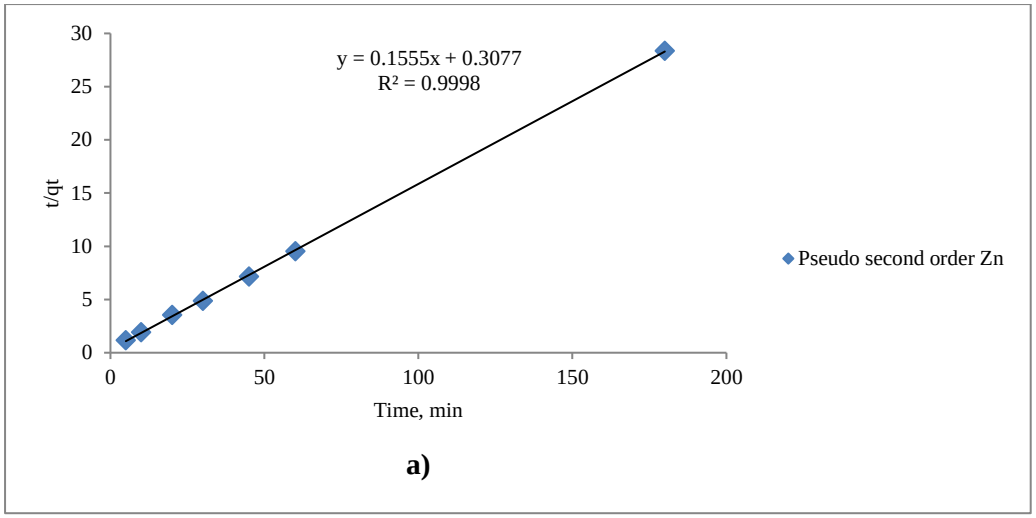

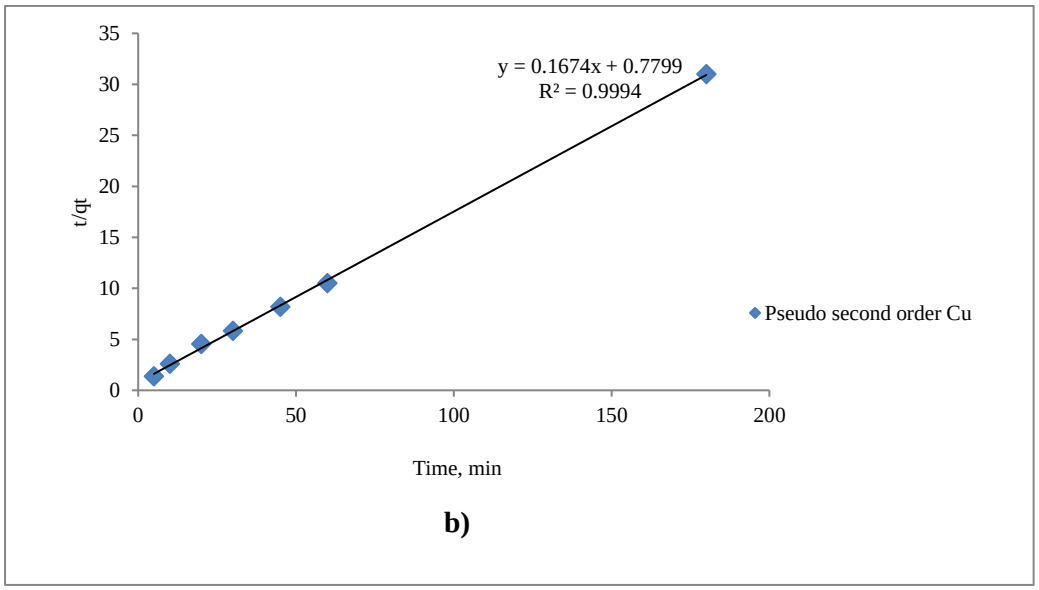

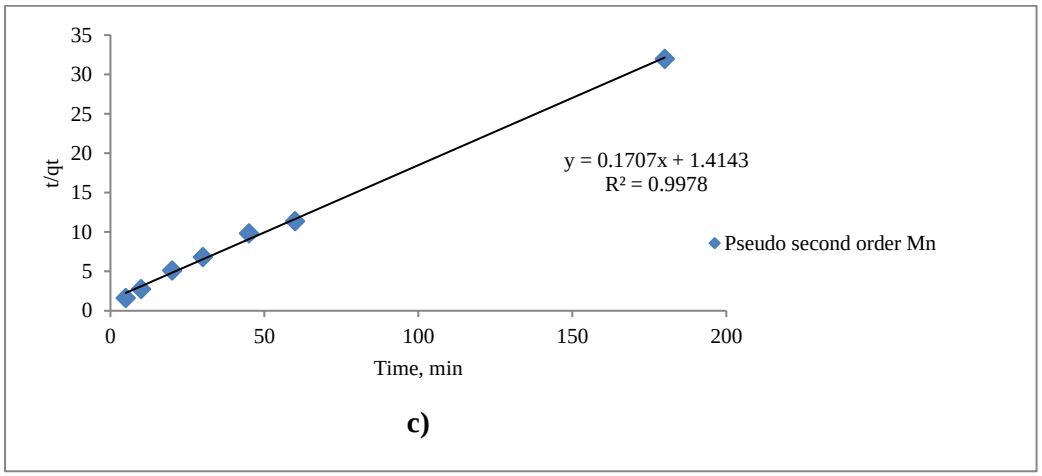

Figure 4.11 Pseudo second order plot for the adsorption of metal ions.

4.1.10 Batch studies: Actual acid mine drainage

Two sets of Kroomdraai decant were used as the case study in this research, one was used as the original sample and the other was fortified with $ZnSO_4 .7H_2O$ and $CuSO_4. 5H_2O$ to achieve the concentration of 33.94 mg/l and 46.01 mg/l respectively. About 1000 mg of banana peel powder having the particle size of 0.4 mm was used to treat fortified and actual AMD from the decant, and thereby investigating its potential as a low cost adsorbent. This section, therefore, gives the findings and discussion on the use of banana peel powder in treating actual and fortified AMD from Kroomdraai decant.

4.1.11 Comparative study

The comparative study was conducted to evaluate the performance of the banana peel powder. The adsorbent was introduced into the initial concentration of a single metal ion component and ternary metal component solutions (composed of Zn, Cu and Mn), fortified AMD and actual AMD. As already stated, the AMD was fortified by Cu ions as $CuSO_4.5H_2O$ and Zn ions as $ZnSO_4.7H_2O$ so as to introduce and increase Cu ions and Zn ion concentrations to the significant amount. Figure 4.12 shows that there is a decrease in percentage removal of Zn and Mn in the fortified AMD compared to the synthetic water. The decrease in percentage removal of Zn, and Mn may be due to the presence of other heavy metals ions competing for the adsorption sites in the banana peel powder. However, the percentage removal of Cu has increased.

In the actual AMD, Mn removal showed a slight increase compared to the fortified AMD. The reasons for this behaviour is not well understood. However, with all the other metals in the AMD kept unchanged the absence of Cu in the actual AMD might have caused this increase, as the banana peel depicted preference for Cu to Mn.

Although Fe is not the metal ion under investigation it was completely removed from the solution at the lowest dosage of 200 mg, which signifies that the adsorbent prefers Fe over other metals under investigation.

The Cd and Al were also significantly removed followed by Ni and Co. The good adsorption of Fe and Al might be because of their high affinity due to their high valence (tri-valence) compared to the competing di-valent metals. This finding is in consistence with the work done

by Kang et al (2004). Although the adsorbent exhibit high adsorption capacity towards Mn in the actual AMD, this indicates that the adsorbent prefers Zn and Cu di-valent ions over Mn (Zn>Cu>Mn).

Overall Figure 4.13 shows that the percentage removal increased with the banana peel powder dosage. This may be caused by the increase in the adsorption site as the banana peel powder dosage is increased. However, Fe, Al showed a strong affinity towards the adsorbent both in the fortified and actual AMD due to that they are trivalent ions. Similar trend were observed on the actual AMD sample as depicted in Figure 4.14, however nickel removal was greater than cadmium.

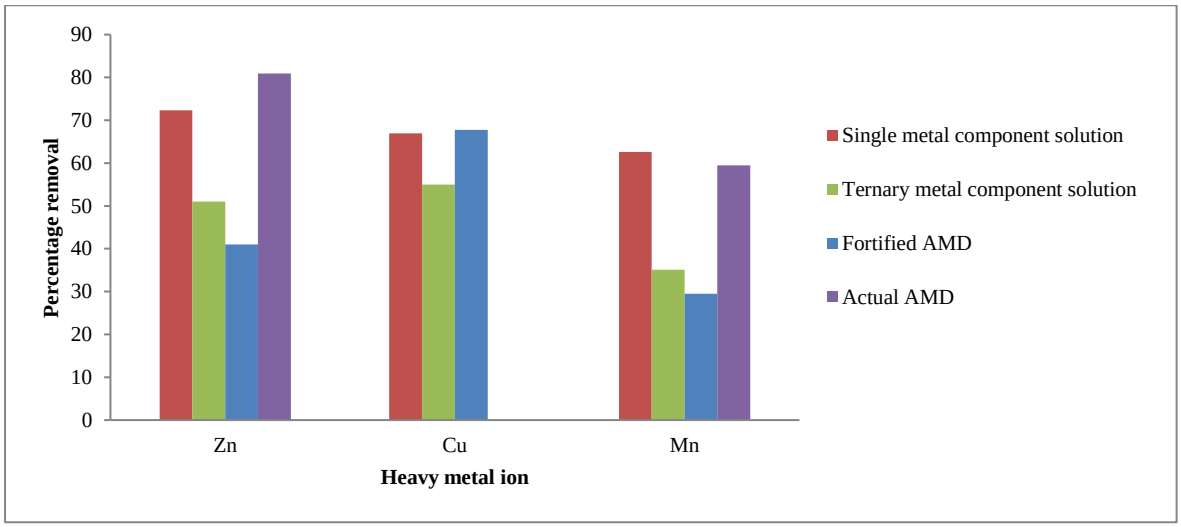

Figure 4.12 Comparisons of adsorption capacities from single component solution, synthetic water solution, fortified AMD and Actual AMD.

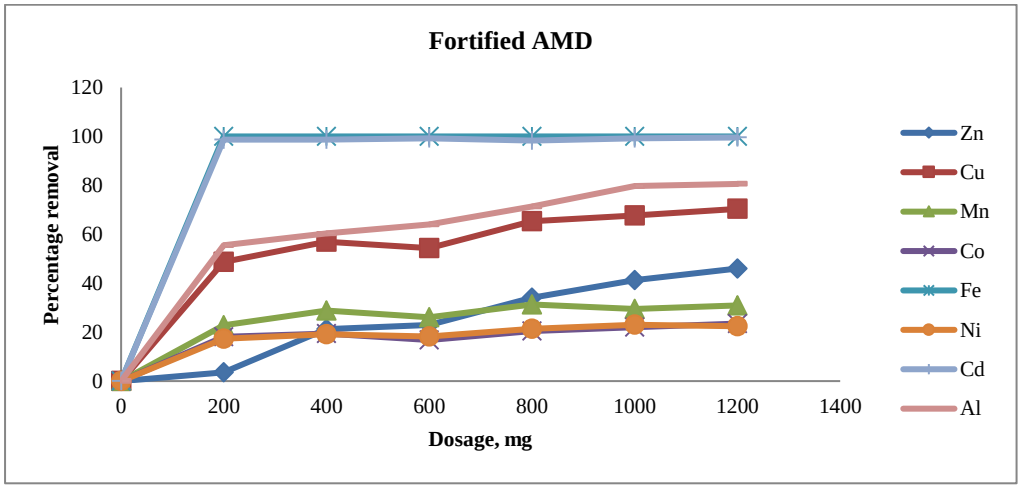

Figure 4.13 Comparisons of adsorption capacities from fortified AMD.

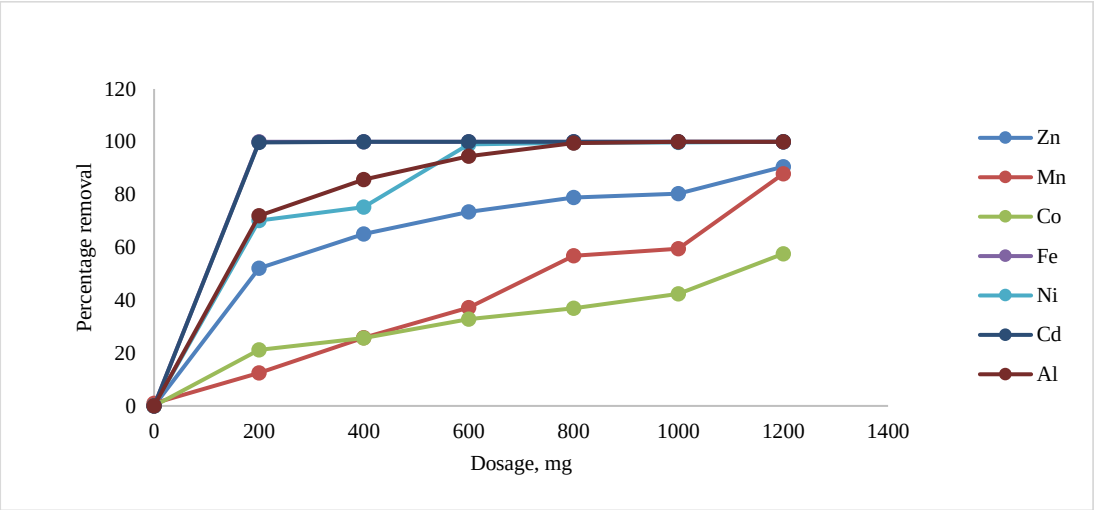

Figure 4.14 Effects of banana peel powder dosage on adsorption of heavy metals from actual AMD

4.2 Column studies- Actual acid mine drainage.

4.2.1 Effect of bed height

The service time of the column increased with the increase in bed depth for both Mn and Zn metal ion as indicated in Figure 4.15. The adsorption capacity of the bed and saturation time increased with increasing bed depth, this may be attributed to more active sites available for binding and longer mass transfer zone. As stated in section 3.2.1, the actual AMD had no Cu metal ions.

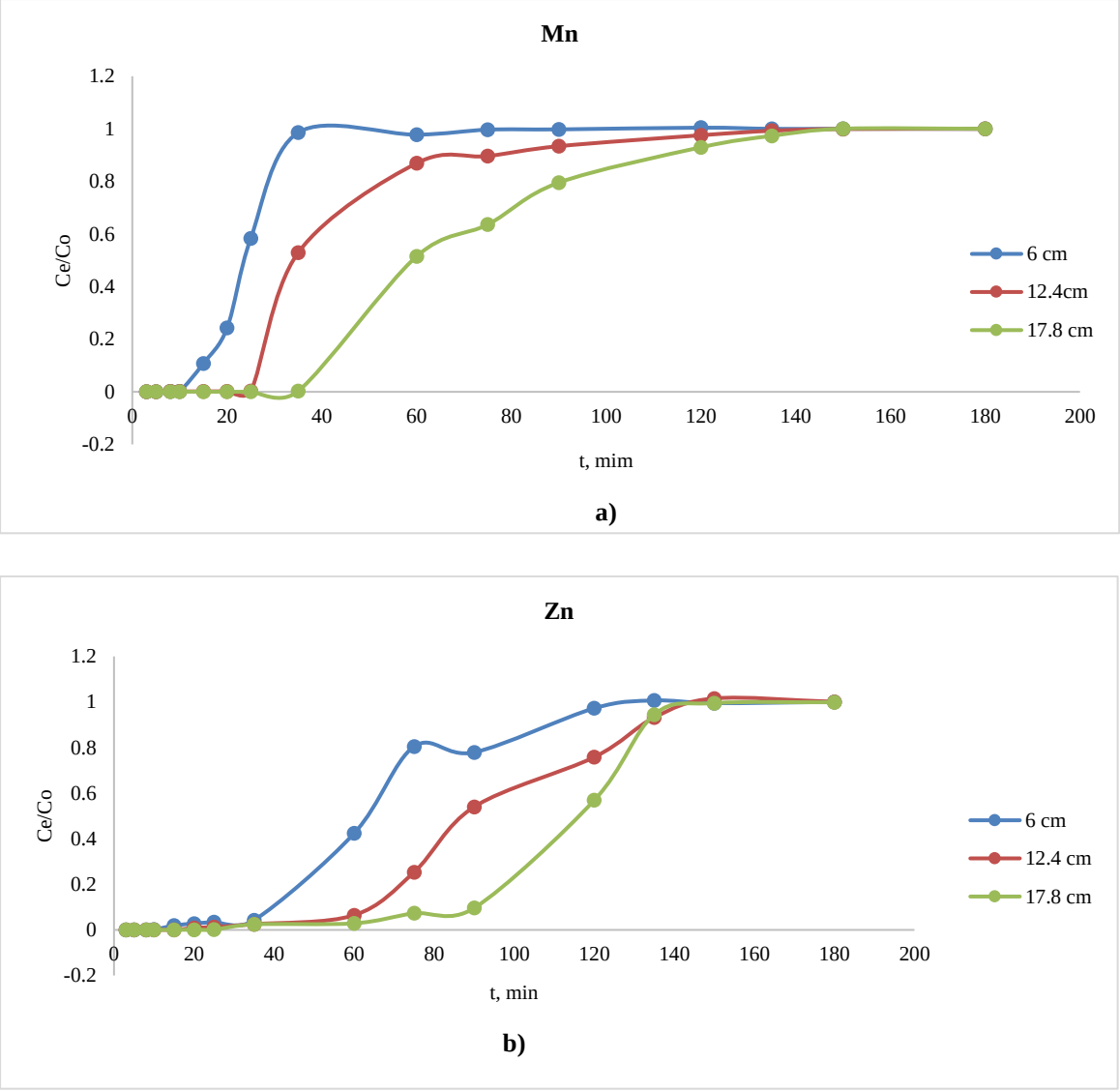

Figure 4.15. The breakthrough curves of Mn (a) and Zn (b) removal by banana peel for different bed depth.

The analysis and modelling of the column data was done using BDST or Bohrat-Adams equation. This model is one of the simple model used to measure the capacity of the bed at different breakthrough values (Vimala et al., 2011). However, the model is based on the surface reaction rate theory, and it neglects the film resistance and the intra-particle mass transfer resistance in such that the metal ions are adsorbed directly onto the surface of the adsorbent.

The model states that the bed depth *(H)* and the service time *(t)* of the column has a linear relationship. The equation is expressed as:

$$t = \frac{N_o H}{C_o v} - \left(\frac{1}{K_a C_o}\right) \ln\left(\frac{C_0}{C_b} - 1\right) - - - - - - - - - - - - - 4.1$$

where C_0 is the initial concentration of solute (mg/L), C_b is the desired concentration of solute at breakthrough point (mg/L), N_o is the adsorption capacity (mg/L), H is the bed depth of the column (cm), K_a is the adsorption rate constant l/(mg.min), t is the service time of column(h) and v is the linear flow velocity of feed to bed (cm/min).

Setting $t = 0$ yields,

$$X_0 = \frac{V}{K C_o} \ln\left(\frac{C_o}{C_b} - 1\right) - - - - - - - - - - - - - - - - - - 4.2$$

where X_0 is the minimum column height necessary to achieve an effluent concentration C_b, known as critical bed depth.

Therefore BDST equation can be expressed as

$$t = aH + b - 4.3$$

where

$$a = slope = \frac{N_o}{C_o v}$$

and

$$b = intercept = -\frac{1}{K_a C_o} \ln\left(\frac{C_0}{C_b} - 1\right)$$

The BDST relation was developed by plotting the data of breakthrough curves for each bed depth of 6, 12.4 and 17.8 cm by recording the service time at 0.2% of initial concentration of each metal ion. Thereafter, the service time (t) was plotted against bed depth (H) at the flow rate of 15 ml/min and was found to be linear as shown in Figure 4.16. The breakthrough point where the effluent concentration is approximately 0.2% of the initial concentration intends to achieve compliance to national water standard for discharge of wastewater to watercourse. The discharge standard for both Mn and Zn is 0.1 mg/L (National Water Act, 2013)

The validity of the BDST model to present the biosorption of heavy metals ions in this study was indicated by the high correlation coefficient values ($R^2 = 1$ and $R^2 = 0.996$ for Mn and Zn respectively).

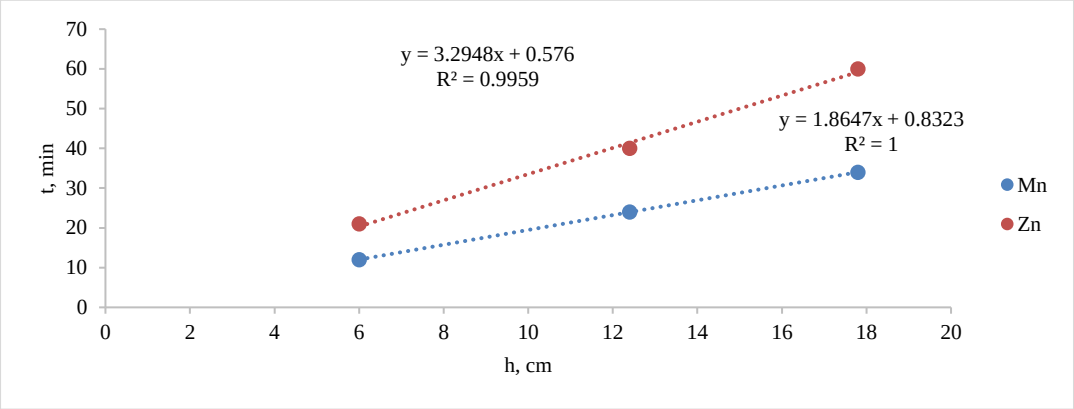

Figure 4.16. BDST plot for Mn and Zn at 15min/mL.

From the intercept and the slope of Figure 4.16 the design parameters like N_o and K_a were found by assuming that the linear flow velocity (v) and concentration (C_o) are constant during the service of the column. The values of N_o, K_a, and X_o were found to be 133.748 mg/l; 0.103 l/(mg.min) and 2.024 cm for Mn, and 18.005 mg/l; 1.772 l/(mg.min) and 0.885 cm for Zn. The rate constant, K_a is a measure of the rate transfer of metal solution from the fluid phase to the solid phase. It influences the breakthrough phenomenon in a column study (Simate and Ndlovu, 2015). When the value of K_a is large the early breakthrough of the bed can be delayed (Vijayaraghavan et al. 2005).The K_a values of Zn is larger than that of Mn and all of its breakthrough point is delayed compared to that of Mn and this finding is in agreement with the batch studies. Therefore, a longer bed depth is recommended for smaller values of K_a to decrease the chances of early breakthrough. The larger the value of N_o and smaller value of X_o indicate high bed capacity for the absorption material. However, the bed capacity will change with service time as the bed depth increases and the residence time with liquid inside the column increases, allowing the adsorbate molecules to diffuse deeper inside the adsorbent.

Table 4.4 indicates the minimum bed height to achieve the desired breakthrough concentration as 2.024 and 0.885 cm for Mn and Zn metal ions respectively, and it shows that the adsorption capacity, N_o was higher for Mn compared to Zn metal ion. This is attributed to the competitive adsorption towards the active site between the heavy metal ions. The high initial concentration of Mn may institute high concentration gradient between the solute and the banana peels.

Table 4.4 The BDST model parameters for the removal of Mn and Zn at 15mL/min

Heavy metal ions	K_a **(L/(mg.min))**	N_o**(mg/L)**	X_o**(cm)**	R^2
Mn	0.103	133.748	2.024	1
Zn	1.772	18.005	0.885	0.996

The BDST model parameters are very useful to scale up the process for different flow rates without further laboratory tests. The ratio of the original and the new flowrates can be multiplied by the slope of the plot of service time against bed depth (Adak and Bandyopadhyay 2006).

The successful design of the adsorption column can also be achieved by using Thomas model to predict the breakthrough profile of the effluent. This model is simple to use and is one of the general and mostly used methods in column performance studies. Thomas model assumes Langmuir kinetics of adsorption-desorption with no axial dispersion and mass transfer kinetics (Fu et al. 2003 and Vijayaraghavan et al. 2005).

The expression of the Thomas model for an adsorption column is as follows:

$$\frac{C_t}{C_o} = \frac{1}{1 + exp\left(\frac{K_{TH}}{Q}\left(q_o M - C_o V_{eff}\right)\right)} \quad ---------- 4.4$$

Where C_o is the initial metal ion concentration (mg/L), C_t is the effluent metal ion concentration (mg/L) at any time (t), q_o is the maximum solid-phase concentration of the solute(mg/g), V_{eff} is the effluent volume (mL), M is the mass of the adsorbent (g), Q is the flow rate (mL/min) and K_{TH} is the Thomas rate constant (mL/mg. min).

The linearized form of the Thomas model is as follows:

$$\ln\left(\frac{C_0}{C_t} - 1\right) = \frac{K_{TH} q_o X}{Q} - \frac{K_{TH} q_o M}{V_{eff}} \quad ---------- 4.5$$

which can be simplified to

$$\ln\left(\frac{C_0}{C_t}-1\right)=\frac{K_{TH}q_oM}{Q}-K_{TH}C_0 \quad ----------4.6$$

The experimental data was fitted into the Thomas model to obtain the kinetic coefficient K_{TH} and adsorption capacity of the bed q_o using regression analysis from a plot in Figure 4.17 of $\ln\left(\frac{C_0}{C_t}-1\right)$ against t at 6, 12.4 and 17.8 cm adsorbent bed and 15 ml/min volumetric flowrate of the influent.

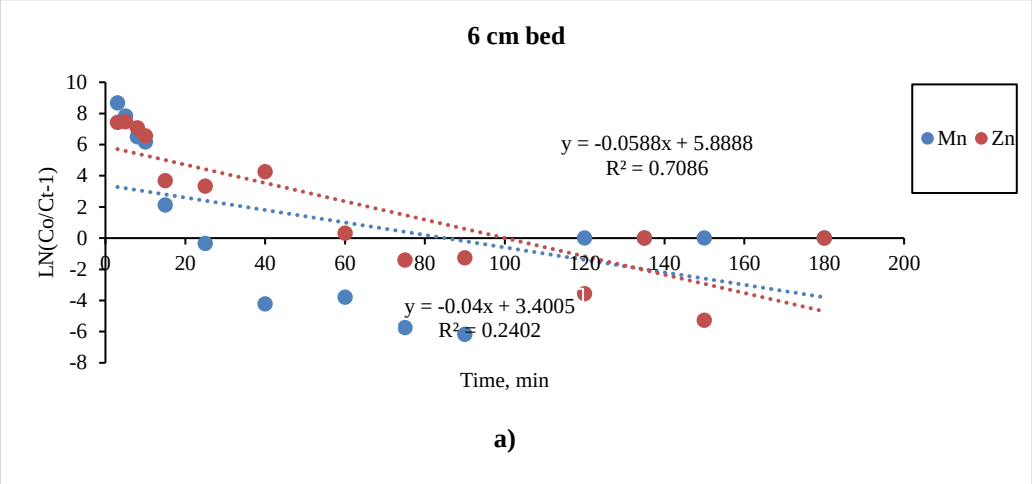

a)

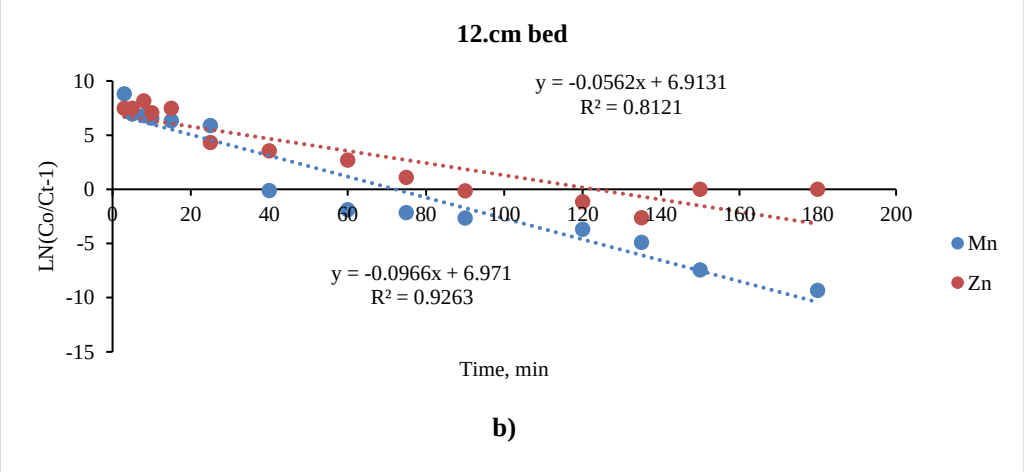

b)

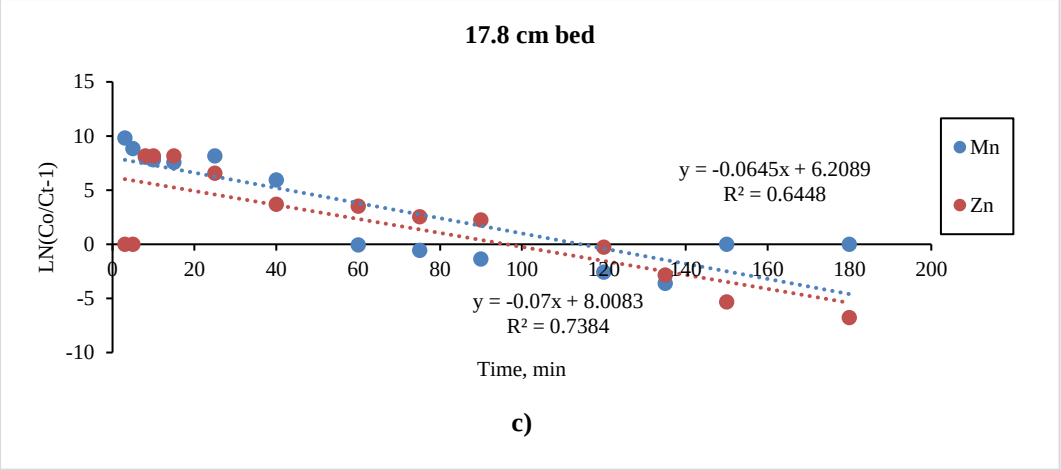

Figure 4.17 Thomas model plot for the removal of Mn and Zn on 17.8 cm adsorption bed and 15 mL/min.

The values of regression coefficient (R^2) presented in Table 4.5 are low and the bed adsorption capacity has a random relationship with the bed depth. The experimental data did not fit well with the Thomas model. This indicates that Thomas model is not appropriate for describing the sorption process for both Mn and Zn. Furthermore, the K_{TH} value decreases with the increase in bed height and is also in agreement with (Chen et al., 2012) but contradicts the studies by (Chowdhury et al., 2013).

Table 4.5 Thomas model parameters for the removal of Mn and Zn on banana peel at different bed depths and flowrates of 15 mL/min.

Metals	**Bed depth (cm)**	q_o **(mg/g)**	K_{TH} **(mL/min mg)**	R^2
Mn	6	5866.500	0.002	0.240
	12.4	2489.913	0.001	0.926
	17.8	2631.586	0.001	0.738
Zn	6	526.537	0.017	0.709
	12.4	323.360	0.016	0.812
	17.8	168.699	0.014	0.649

4.2.2 Effect of flowrates

The effect of the actual AMD flowrate on the adsorption of Mn and Zn on banana peel adsorbent was studied by varying the influent flowrate (15, 30 and 45 ml/min) with the constant adsorbent bed depth of 17.8 cm, inlet concentration of 46.006 and 3.505 mg/L for Mn and Zn, respectively. The Mn breakthrough curves in Figure 4.18 show that for flowrate of 15 mL/min the adsorption bed takes longer to reach breakthrough point (~ 33 minutes) compared to about 15 and 4 minutes taken at flow rates of 30 and 45 mL/min, respectively.

The breakthrough point for Zn (Figure 4.19) was at 60, 25 and 15 minutes for 15mL/min, 30mL/min and 45 mL/min, respectively. Lower flow rate has resulted in longer residence time of the liquid which allows for more contact time between the metal ions and the adsorbent. However, the high flowrates led to the reduction of metal ion uptake. This reduction is probably due to the unavailability of sufficient contact time for solute to interact with the sorbent and the limited diffusivity of solute into the sorptive sites or pores. This is in agreement with the work done by Han et al (2009), Hasfalina et al (2012) and Chao et al (2014).

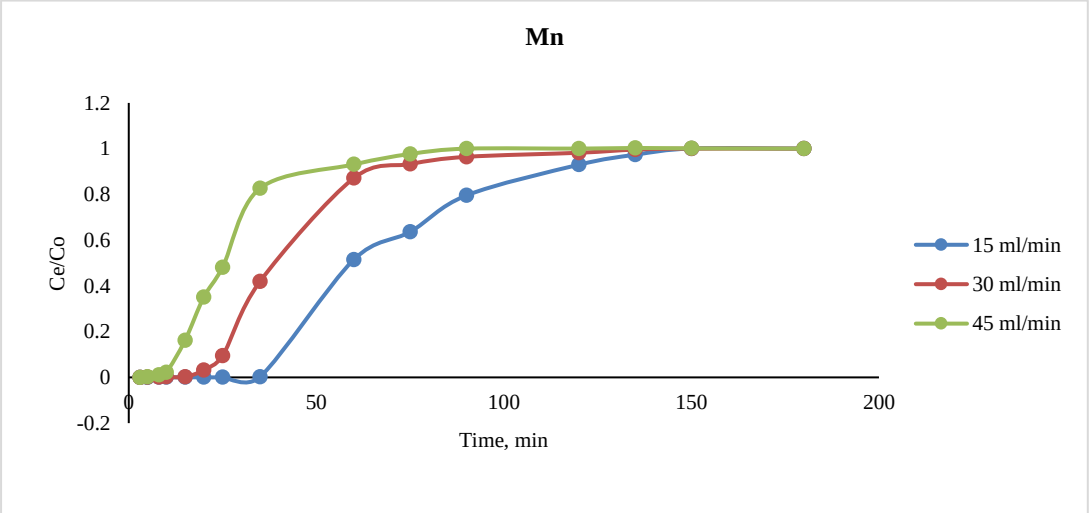

Figure 4.18 Breakthrough curve for Mn removal at 17.8 cm and different influent flowrate.

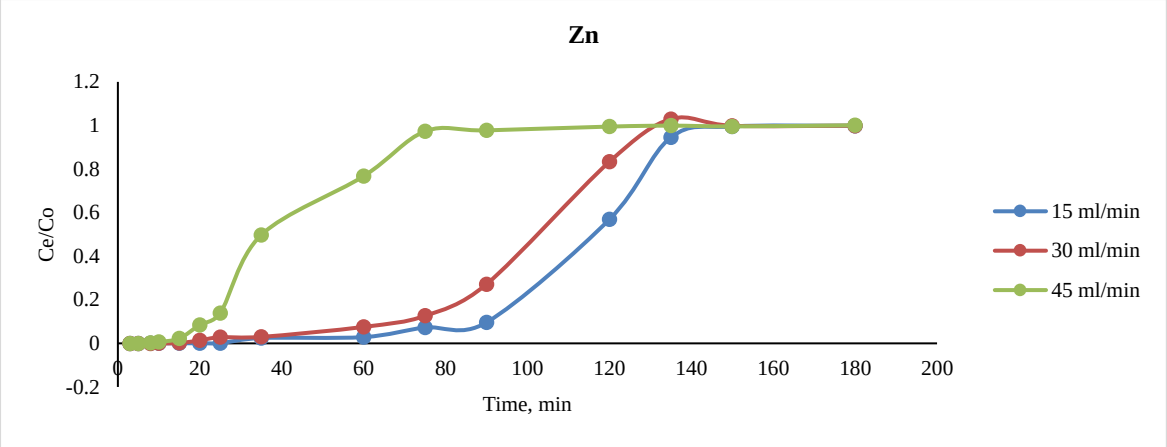

Figure 4.19 Breakthrough curve for Zn removal at 17.8 cm and different influent flowrate.

The BDST relation was developed by plotting the data of breakthrough curves for each flowrate of 15, 30 and 45 mL/min by recording the service time to reach 0.2% of initial concentration. Thereafter, the service time (t) was plotted against linear velocity at the bed depth of 17.8 cm and was found to be linear as shown in Figure 4.20.

The validity of the BDST model to present the biosorption of heavy metals ions in this study was indicated by the high correlation coefficient values ($R^2 = 0.984$ and $R^2 = 0.999$ for Mn and Zn, respectively).

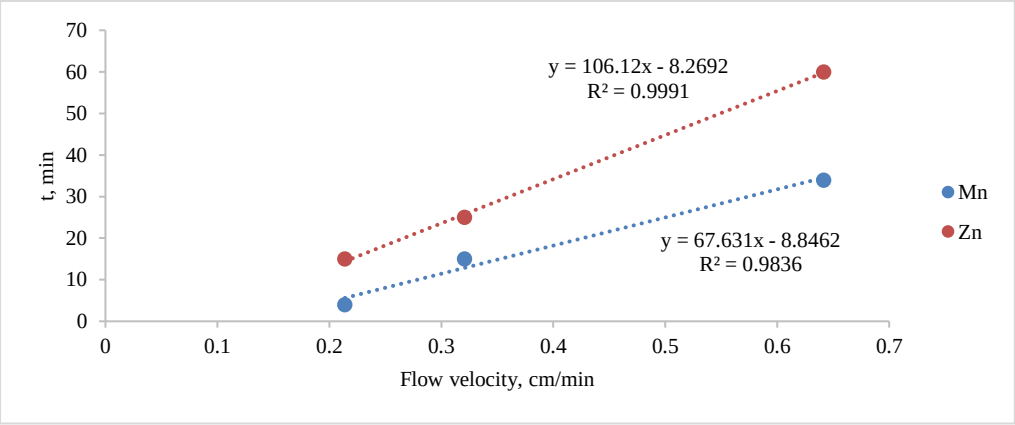

Figure 4.20 BDST plot for Zn and Mn at 17.8 cm

From the intercept and the slope, the design parameters like N_o and K_a as listed in Table 4.6 were found for the constant bed depth (H) and initial concentration (C_o).

Table 4.6 The BDST model parameters for the removal of Mn and Zn at 17.8 cm

Heavy metal ions	K_a (L/(mg.min))	N_o(mg/L)	R^2
Mn	0.015	112.132	0.984
Zn	0.021	13.469	0.991

The high correlation coefficient values (R^2 = 0.984 and R^2 =0.999) for Mn and Zn, respectively) indicates the validity of the BDST model to present the removal of heavy metals ion in this study. It can also be seen that the value of K_a was higher for Zn compared to Mn. This can be attributed to the high availability of Zn metal ions in the bulk solute due to its low hydrolysis constant compared to the Mn that has high hydrolysis constant. However the value of N_o for Zn is smaller compared to that for Mn. This can be attributed to the lower initial concentration of Zn in the actual AMD compared to that of Mn, and this may lead to more adsorption of Mn due to high concentration gradient between the solute and surface of the banana peels. These results are in agreement with the findings of the batch studies in section 4.1.6.

The experimental data was also fitted to Thomas model by plotting $\ln\left(\frac{C_0}{C_t}-1\right)$ against t at different flow rates (15, 30, 45 mL/min). The relative coefficients and constants were obtained using linear regression analysis according to equation 4.6 and the results are listed in Table 4.7.

Table 4.7 Thomas model parameters for the removal of Mn and Zn on banana peel at different flowrates and constant bed depth17.8 cm.

Metals	Flowrate (mL/min)	q_o (mg/g)	K_{TH} (mL/min mg)	R^2
Mn	15	1993.318	0.002	0.929
	30	27652.484	0.0003	0.938
	45	3945.964	0.001	0.781
Zn	15	523.643	0.017	0.750
	30	671.842	0.008	0.188
	45	233.732	0.022	0.386

The results show that q_o values for Zn decreased with the increase in flow rates which is agreement with Simate and Ndlovu (2015) on similar studies, but reverse trend was observed for Mn, where K_{TH} values were random with each flow rates and depict no trend with the flow rates. The correlation coefficient as read from Figure 4.21 ranges from 0.188 to 0.750 and 0.781 to 0.938 for Zn and Mn, respectively. This coefficient indicates that the Thomas model is not the best fit for this study.

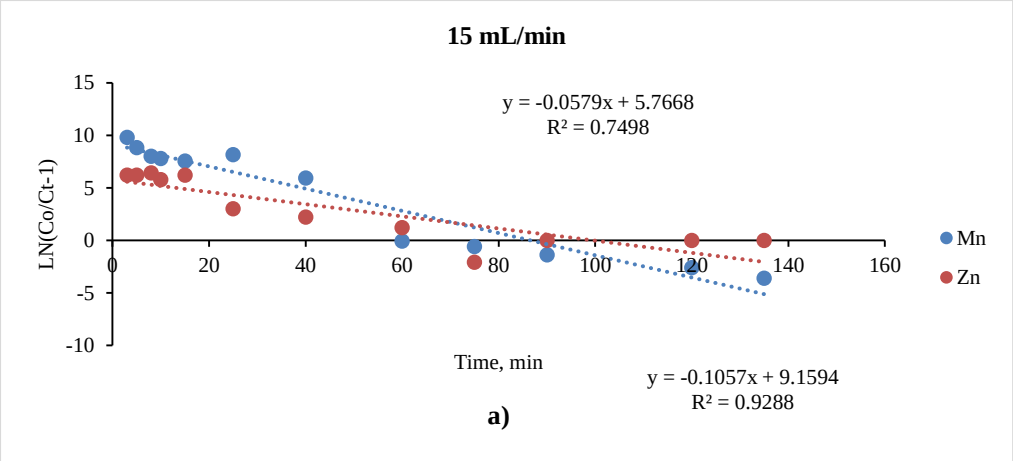

a)

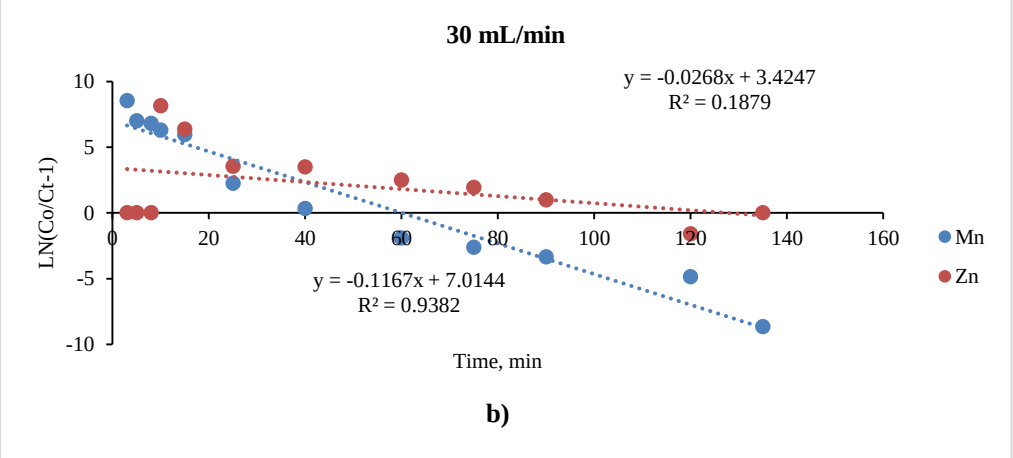

b)

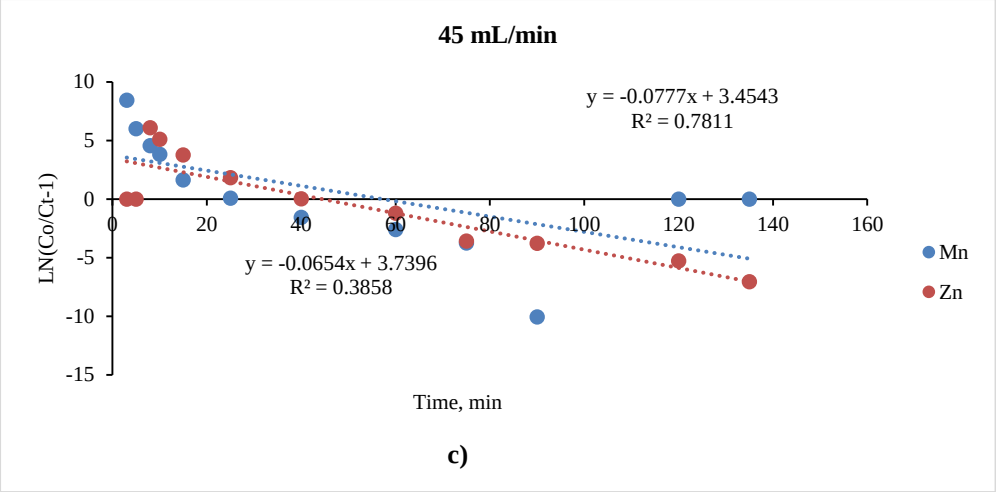

Figure 4.21 Thomas model plot for the removal of Mn and Zn on 17.8 cm adsorption bed

CHAPTER 5

5. CONCLUSION AND RECOMMENDATIONS

5.1 Conclusions

The main objective of the study was to explore the adsorption potential of banana peels as low cost adsorbent for heavy metals under synthetic water, actual AMD and fortified AMD conditions. The effects of particle size, contact time, mass loading, initial concentration, selectivity and pH were studied for each metal ion under investigation. The morphological transformation of the banana peel was also investigated. The metal rention of the banana peels from actual AMD was investigated in a fixed bed configurations at different flow rates and bed depth.

The following conclusions were drawn from this research work:

The contact time to reach saturation were 30 minutes for Cu and Zn, and about 60 minutes for Mn under single component solution. More than 70% of Zn and more than 60% of Cu and Mn per 1000 mg of banana peel in a single metal component solution were removed. The amount of heavy metals ion removed decreased in the fortified and actual AMD environment.

Under fortified AMD conditions 41.08, 67.74 and 29.52% per 1000mg of banana peel for Zn, Cu and Mn ion, respectively, were removed. However, the percentage of Mn (59.49 % per 1000mg) adsorbed from actual AMD condition showed a slight increase compare to its removal under ternary solution (35.07%).

The adsorption process for all the metal ions under investigation in the single component solution fitted the Langmuir isotherm and Frendlich model, and according to Langmuir isotherm, the adsorption capacity for Zn, Cu and Mn were 9.01, 8.72 and 6.92 mg/g, respectively. The removal percentage of Zn, Cu and Mn increased with the increase in pH. The increase in particle size showed poor adsorption for all the metal ions under investigation. The removal efficiency increased with the increase in mass dosage of the banana peels. Rough surface texture and porosity could be distinctly noticed after adsorption and the banana peel became less compacted.

The relatively long adsorbent bed depth delayed a breakthrough point. The relatively high flow rates resulted to quicker breakthrough points. The experimental data best fitted BDST model than Thomas model for all conditions investigated.

Adsorbent bed depth investigated in this study could remove Mn and Zn to meet the effluent standard of 0.1 mg/L for both Mn and Zn. The volume of water treated to remove Mn ion concentration from 46.01 mg/L to the effluent standard (0.1 mg/L) at 15mL/min at the bed depth of 6, 12.4, and 17.8 cm was 180, 360 and 510 mL, respectively. The volume of water to remove Zn from 3.505 mg/L to 0.1 mg/L at the bed depth of 6, 12.4 and 17.8 cm was 315, 600, 900 mL, respectively.

It is therefore concluded that banana peel can be used as a cheap adsorbent to remove the Zn, Cu and Mn under AMD conditions.

5.2 Recommendations

Future studies must be conducted to study desorption or regeneration of the banana peel powder using different leaching agents, for potential re-use. The banana peel powder adsorption potential should be investigated on different AMD sources other than one decant point from coal mine.

6. REFERENCES

1. Abollino, O., Aceto, M., Malandrino, M., Sarzanini, C. & Mentasti, E. 2003, "Adsorption of heavy metals on Na-montmorillonite. Effect of pH and organic substances", Water research, 37(7), pp 1619-1627.
2. Adak, A., Bandyopadhyay, M. & Pal, A. 2006, Fixed bed column study for the removal of crystal violet (CI Basic Violet 3) dye from aquatic environment by surfactant-modified alumina, *Dyes and Pigments*, 69(3), pp 245-251.
3. Akcil, A. and Koldas, S., 2006. Acid Mine Drainage (AMD): causes, treatment and case studies. *Journal of Cleaner Production*, 14(12), pp 1139-1145.
4. Akmil-Başar, C., Önal, Y., Kılıçer, T. and Eren, D., 2005. Adsorptions of high concentration malachite green by two activated carbons having different porous structures. *Journal of hazardous materials*, 127(1), pp 73-80.
5. Al-Azzawi, M., Shartooh, S. and Al-Hiyaly, S., 2013. The removal of zinc, chromium and nickel from industrial waste water using banana peels. *Iraqi Journal of Science*, 54(1), pp 72-81.
6. Ali, I. 2012, New generation adsorbents for water treatment, *Chemical reviews*, 112(10), pp 5073-5091.
7. Al-Asheh, S. and Duvnjak, Z., 1995. Adsorption of copper and chromium by Aspergillus carbonarius. *Biotechnology Progress*, 11(6), pp.638-642.
8. Anwar, J., Shafique, U., Salman, M., Dar, A. and Anwar, S., 2010. Removal of Pb (II) and Cd (II) from water by adsorption on peels of banana. *Bioresource technology*, *101*(6), pp 1752-1755.
9. Ashton, P.J., Love, D., Mahachi, H. and Dirks, P., 2001. An overview of the impact of mining and mineral processing operations on water resources and water quality in the Zambezi, Limpopo and Olifants Catchments in Southern Africa. *Contract Report to the Mining, Minerals and Sustainable Development (Southern Africa) Project, by CSIR-Environmentek, Pretoria and Geology Department, University of Zimbabwe-Harare.Report No.ENV-PC*, 42.
10. Bajpai, A. and Rajpoot, M., 1999. Adsorption Techniques - A Review. *Journal of Scientific & Industrial Research*, 58, pp 884-860.
11. Barnes, H. and Romberger, S., 1968. Chemical aspects of acid mine drainage. *Journal (Water Pollution Control Federation)*, 40(3), pp 371-384.

12. Bell, F., Bullock, S., Hälbich, T. and Lindsay, P., 2001. Environmental impacts associated with an abandoned mine in the Witbank Coalfield, South Africa. *International Journal of Coal Geology*, 45(2), pp 195-216.
13. Buekens, A. and Zyaykina, N., 2001. Adsorbents and Adsorption Processes for Pollution Control. *Pollution Control Technologies,* 2.
14. Bullen, C., Coulton, R., Dolan, J., Hallett, C., Marsden, C. & Wright, J. 2003. Wheal Jane mine water active treatment plant- design, construction and operation, *Land Contamination & Reclamation,* 11 (2), pp 245-252.
15. Chao, H.P., Chang, C.C. and Nieva, A., 2014. Biosorption of heavy metals on Citrus maxima peel, passion fruit shell, and sugarcane bagasse in a fixed-bed column. *Journal of Industrial and Engineering Chemistry*, *20*(5), pp 3408-3414.
16. Chen, S., Yue, Q., Gao, B., Li, Q., Xu, X. & Fu, K. 2012, "Adsorption of hexavalent chromium from aqueous solution by modified corn stalk: a fixed-bed column study, *Bioresource technology,* (113), pp 114-120.
17. Chowdhury, Z., Zain, S., Rashid, A., Rafique, R. & Khalid, K. 2012.Breakthrough curve analysis for column dynamics sorption of Mn (II) ions from wastewater by using Mangostana garcinia peel-based granular-activated carbon, *Journal of chemistry*, 2013.
18. Clarke, W.A., Konhauser, K.O., Thomas, J.C. and Bottrell, S.H., 1997. Ferric hydroxide and ferric hydroxysulfate precipitation by bacteria in an acid mine drainage lagoon. *FEMS Microbiology Reviews*, 20(3-4), pp 351-361.
19. Coetzee, H., Hobbs, P., Burgess, J., Thomas, A., Keet, M., Yibas, B., Van Tonder, D., Netili, F., Rust, V. and Wade, P., 2010. Mine water management in the Witwatersrand Gold Fields with special emphasis on acid mine drainage. *Report to the Inter-Ministerial Committee on Acid Mine Drainage*.
20. Department of Water Affairs, 2013. Revision of general authorisations in terms of Section 39 of the National Water Act, 1998 (Act No. 36 of 1998), No. 665. *Government Gazette*, (36820).
21. Deshmukh, P.D., Khadse, G.K., Shinde, V.M. and Labhasetwar, P., 2017. Cadmium Removal from Aqueous Solutions Using Dried Banana Peels as An Adsorbent: Kinetics and Equilibrium Modeling. *J Bioremediat Biodegrad*, *8*(395), pp 2.
22. da Silveira, A.N., Silva, R. & Rubio, J. 2009. Treatment of acid mine drainage (AMD) in South Brazil: comparative active processes and water reuse", International Journal of Mineral Processing, 93(2), pp 103-109.

23. Demchak, J., Morrow, T. and Skousen, J., 2001. Treatment of acid mine drainage by four vertical flow wetlands in Pennsylvania. *Geochemistry: Exploration, Environment, Analysis,* 1(1), pp 71-80.
24. Elliot Martin, A., 1981. Chemistry of coal utilization, 2nd supplementary volume.
25. Falayi, T. and Ntuli, F., 2014. Removal of heavy metals and neutralisation of acid mine drainage with un-activated attapulgite. Journal of industrial and Engineering Chemistry, 20(4), pp 1285-1292.
26. Fu, Y. & Viraraghavan, T. 2003. Column studies for biosorption of dyes from aqueous solutions on immobilised Aspergillus niger fungal biomass, Water Sa, vol. 29(4), pp. 465-472.
27. Giwa, A., Bello, I., Oladipo, M. and Adeoye, D., 2013. Removal of cadmium from waste-water by adsorption using the husk of melon (Citrullus lanatus) Seed. *International Journal of Basic and Applied Sciences,* 2(1), pp. 110-123.
28. Griffiths, P.R. and De Haseth, J.A., 2007. *Fourier transform infrared spectrometry* , 171. John Wiley & Sons.
29. Grzybkowski, W., 2006. Nature and Properties of Metal Cations in Aqueous Solutions. *Polish Journal of Environmental Studies*, *15*(4).
30. Gunatilake, S., 2015. Methods of removing heavy metals from industrial wastewater. *Journal of Multidisciplinary Engineering Science Studies,* 1(1), pp. 12-18.
31. Han, R., Wang, Y., Zhao, X., Wang, Y., Xie, F., Cheng, J. & Tang, M. 2009. Adsorption of methylene blue by phoenix tree leaf powder in a fixed-bed column: experiments and prediction of breakthrough curves, Desalination, 245(1-3), pp. 284-297.
32. Hasfalina, C.M., Maryam, R.Z., Luqman, C.A. and Rashid, M., 2012. Adsorption of copper (II) from aqueous medium in fixed-bed column by kenaf fibres. *APCBEE procedia*, *3*, pp.255-263.
33. Hartman, H.L., Mutmansky, J.M., Ramani, R.V. and Wang, Y.J., 2012. *Mine ventilation and air conditioning*. John Wiley & Sons.
34. Harun-Or-Rashid, H., Urbi, Z. and Islam, M., 2014. Environmental impact of coal mining: a case study on the Barapukuria coal mining industry, Dinajpur, Bangladesh. *Middle-East Journal of Scientific Research,* 21(1), pp 268-274.
35. Hossain, M., Ngo, H.H., Guo, W. and Nguyen, T., 2012. Removal of copper from water by adsorption onto banana peel as bioadsorbent. *International Journal of Geomate,* 2(2), pp. 227-234.

36. Iqbal, M. and Edyvean, R.G.J., 2004. Biosorption of lead, copper and zinc ions on loofa sponge immobilized biomass of Phanerochaete chrysosporium. *Minerals Engineering*, 17(2), pp.217-223.
37. Jain, C.K., Malik, D.S. and Yadav, A.K., 2016. Applicability of plant based biosorbents in the removal of heavy metals: a review. *Environmental Processes*, *3*(2), pp 495-523.
38. Jennings, S.R., Blicker, P.S. and Neuman, D.R., 2008. *Acid mine drainage and effects on fish health and ecology: a review:* Reclamation Research Group.
39. Jennings, S.R., Dollhopf, D.J. and Inskeep, W.P., 2000. Acid production from sulfide minerals using hydrogen peroxide weathering. *Applied Geochemistry,* 15(2), pp 235-243.
40. Johnson, D.B. and Hallberg, K.B., 2005. Acid mine drainage remediation options: a review. *Science of the total environment,* 338(1), pp 3-14.
41. Johnson, D.B., 2003. Chemical and microbiological characteristics of mineral spoils and drainage waters at abandoned coal and metal mines. *Water, Air and Soil Pollution: Focus,* 3(1), pp. 47-66.
42. Kang, S.Y., Lee, J.U., Moon, S.H. and Kim, K.W., 2004. Competitive adsorption characteristics of Co 2+, Ni 2+, and Cr 3+ by IRN-77 cation exchange resin in synthesized wastewater. *Chemosphere*, *56*(2), pp. 141-147.
43. Kanyal, M. and Bhatt, A.A., 2015. Removal of heavy metals from water (Cu and Pb) using household waste as an adsorbent. *Journal of Bioremediation and Biodegredation*, *6*(1), p.1.
44. Kibria, M.G., Quamruzzaman, C., Ullah, A.W. and Kabir, A.F., 2012. Effect of longwall mining on groundwater for underground coal extraction in Barapukuria, Bangladesh. *Journal of Mines, Metals and Fuels*, 60, pp 60-66.
45. Kirby, D., 2014. Effective Treatment Options for Acid Mine Drainage in the Coal Region of West Virginia.
46. Vasanth Kumar, K., Subanandam, K., Ramamurthi, V. and Sivanesan, S., 2004. Solid-liquid adsorption for wastewater treatment: principle design and operation.
47. Lemley, A., Wagenet, L. and Kneen, B., 1995. *Activated Carbon Treatment of Drinking Water:* Cornell Cooperative Extension, New York State College of Human Ecology.

48. Lin, S. and Juang, R., 2002. Heavy metal removal from water by sorption using surfactant-modified montmorillonite. *Journal of hazardous materials,* 92(3), pp. 315-326.
49. Makgae, M., McCullough, C., Lund, M. and Wyses, L., 2012. The status and implications of the AMD legacy facing South Africa, *International Mine Water Association Symposium,* 2012, pp. 327-334.
50. Margeta, K., Farkas, A., Šiljeg, M. and Logar, N.Z., 2013. *Natural zeolites in water treatment-how effective is their use:* INTECH Open Access Publisher.
51. Mattson, J.S. and Mark, H.B., 1971. *Activated carbon: surface chemistry and adsorption from solution:* M. Dekker.
52. Mavrov, V., Stamenov, S., Todorova, E., Chmiel, H. and Erwe, T., 2006. New hybrid electrocoagulation membrane process for removing selenium from industrial wastewater. *Desalination,* 201(1-3), pp 290-296.
53. McCarthy, T.S. and Humphries, M.S., 2013. Contamination of the water supply to the town of Carolina, Mpumalanga, January 2012. *South African Journal of Science,* 109(9-10), 01-10.
54. McCarthy, T.S., 2011. The impact of acid mine drainage in South Africa. *South African Journal of Science,* 107(5-6), pp 01-07.
55. Meena, A.K., Kadirvelu, K., Mishra, G., Rajagopal, C. and Nagar, P., 2008. Adsorptive removal of heavy metals from aqueous solution by treated sawdust (Acacia arabica). *Journal of hazardous materials,* 150(3), pp 604-611.
56. Metesh, J.J., Jarrell, T. and Oravetz, S., 1998. *Treating acid mine drainage from abandoned mines in remote areas:* USDA Forest Service, Technology and Development Program.
57. Mitchell James, K., 1993. Fundamentals of soil behavior.
58. Mohan, S. & Sreelakshmi, G. 2008. Fixed bed column study for heavy metal removal using phosphate treated rice husk, *Journal of hazardous materials*, 153(1), pp 75-82.
59. Montanher, S., Oliveira, E. and Rollemberg, M., 2005. Removal of metal ions from aqueous solutions by sorption onto rice bran. *Journal of hazardous materials*, pp 117(2), 207-211.
60. Moreno, J.C., Gómez, R. and Giraldo, L., 2010. Removal of Mn, Fe, Ni and Cu ions from wastewater using cow bone charcoal. *Materials*, *3*(1), pp 452-466.
61. Mudd, G.M. and Ali, S.H., Social and Ecological Impact of Water Extraction for a Copper-Uranium Mine.

62. Naicker, K., Cukrowska, E. and McCarthy, T., 2003. Acid mine drainage arising from gold mining activity in Johannesburg, South Africa and environs. *Environmental pollution*, 122(1), pp 29-40.
63. Neto, V.D.O.S., Raulino, G.S.C., Paulo de Tarso, C.F., Araújo-Silva, M.A. and do Nascimento, R.F., 2013. Equilibrium and kinetic studies in adsorption of toxic metal ions for wastewater treatment. *Viewpoints*, 7, p.8.
64. Neto, V.D.O.S., Raulino, G.S.C., Paulo de Tarso, C.F., Araújo-Silva, M.A. and do Nascimento, R.F., 2013. Equilibrium and kinetic studies in adsorption of toxic metal ions for wastewater treatment. *viewpoints*, *7*, p.8.
65. Pinnavaia, T.J., 1983. Intercalated clay catalysts. *Science*, *220*(4595), pp.365-371.
66. Ramani, R.V., 1992. Mine ventilation. *SME Mining Engineering Handbook,* 2, pp 1068.
67. Reed, S.J.B., 2005. *Electron microprobe analysis and scanning electron microscopy in geology*. Cambridge University Press.
68. Riley, C.V., 1960. The ecology of water areas associated with coal strip-mined lands in Ohio. *The Ohio Journal of Science*, 60(2), pp106-121
69. Reddy, N.A., Lakshmipathy, R. and Sarada, N.C., 2014. Application of Citrullus lanatus rind as biosorbent for removal of trivalent chromium from aqueous solution. *Alexandria Engineering Journal*, *53*(4), pp.969-975.
70. Simate, G.S. and Ndlovu, S., 2014. Acid mine drainage: Challenges and opportunities. *Journal of Environmental Chemical Engineering*, 2(3), 1785-1803.
71. Simate, G.S. and Ndlovu, S., 2015. The removal of heavy metals in a packed bed column using immobilized cassava peel waste biomass. *Journal of Industrial and Engineering Chemistry*, 21, pp 635-643.
72. Skousen, J. and Ziemkiewicz, P., 2005. Performance of 116 passive treatment systems for acid mine drainage. *Proceedings, American Society of Mining and Reclamation, Breckenridge, CO*, pp 1100-1133.
73. Somorjai, G.A., 1994. The surface science of heterogeneous catalysis. *Surface science*, *299*, pp 849-866.
74. Srinivasan, R., 2011. Advances in application of natural clay and its composites in removal of biological, organic, and inorganic contaminants from drinking water. *Advances in Materials Science and Engineering*, 2011, pp 1-17.

75. Stilwell, L., Minnitt, R., Monson, T. and Kuhn, G., 2000. An input–output analysis of the impact of mining on the South African economy. *Resources Policy*, 26(1), pp 17-30.
76. Sud, D., Mahajan, G. and Kaur, M., 2008. Agricultural waste material as potential adsorbent for sequestering heavy metal ions from aqueous solutions–A review. *Bioresource technology*, 99(14), pp 6017-6027.
77. Takahashi, M., Muroi, M., Inoue, A., Aoki, M., Takizawa, M., Ishigure, K. and Fujita, N., 1987. Properties of bentonite clay as buffer material in high-level waste geological disposal. Part I: Chemical species contained in bentonite. *Nuclear Technology*, 76(2), pp 221-228.
78. Taylor, J., Pape, S. and Murphy, N., 2005. A summary of passive and active treatment technologies for acid and metalliferous drainage (AMD), *5th Australian workshop on Acid Mine Drainage*, Fremantle, Australia.
79. Tutu, H., McCarthy, T. and Cukrowska, E., 2008. The chemical characteristics of acid mine drainage with particular reference to sources, distribution and remediation: The Witwatersrand Basin, South Africa as a case study. *Applied Geochemistry*, 23(12), pp 3666-3684.
80. Valente, T.M. and Gomes, C.L., 2009. Occurrence, properties and pollution potential of environmental minerals in acid mine drainage. *Science of the Total Environment*, 407(3), pp 1135-1152.
81. van Wyk, E., Mokgatle, T. and de Meillon, N., Witwatersrand Mine Voids – Their Hydrochemistry and Hydrodynamic Characteristics.
82. Veli, S. and Alyüz, B., 2007. Adsorption of copper and zinc from aqueous solutions by using natural clay. *Journal of hazardous materials*, *149*(1), pp 226-233.
83. Vijayaraghavan, K., Jegan, J., Palanivelu, K. & Velan, M. 2005. Batch and column removal of copper from aqueous solution using a brown marine alga Turbinaria ornata, *Chemical Engineering Journal*, 106(2), pp 177-184.
84. Vimala, R., Charumathi, D. & Das, N. 2011. Packed bed column studies on Cd (II) removal from industrial wastewater by macrofungus Pleurotus platypus, *Desalination*, 275(1), pp 291-296.
85. Wu, Y., Zhou, J., Wen, Y., Jiang, L. and Wu, Y., 2012. Biosorption of heavy metal ions ($Cu2^{+}$, $Mn2^{+}$, $Zn2^{+}$, and $Fe3^{+}$) from aqueous solutions using activated sludge: Comparison of aerobic activated sludge with anaerobic activated sludge. *Applied biochemistry and biotechnology*, *168*(8), pp.2079-2093.

86. Werdmüller, V., 1986. The central rand. *Witwatersrand Gold—100 Years*, pp 7-47.
87. Worch, E., 2012. *Adsorption technology in water treatment: fundamentals, processes, and modeling:* Walter de Gruyter.
88. Younger, P.L., Banwart, S.A. and Hedin, R.S., 2002. Mine Water Hydrology. *Mine Water*. Springer, pp 127-270. 7
89.
90. Yu, B., Zhang, Y., Shukla, A., Shukla, S.S. & Dorris, K.L. 2001. The removal of heavy metals from aqueous solutions by sawdust adsorption—removal of lead and comparison of its adsorption with copper, *Journal of hazardous materials*, 84(1), pp 83-94.
91. Zhang, Y., Zhao, J., Jiang, Z., Shan, D. and Lu, Y., 2014. Biosorption of Fe (II) and Mn (II) ions from aqueous solution by rice husk ash. *Biomed research international*, *2014*.
92. Zhengfu, B., Inyang, H.I., Daniels, J.L., Frank, O. & Struthers, S. 2010. Environmental issues from coal mining and their solutions, *Mining Science and Technology (China*), 20(2), pp. 215-223.

APPENDIX A

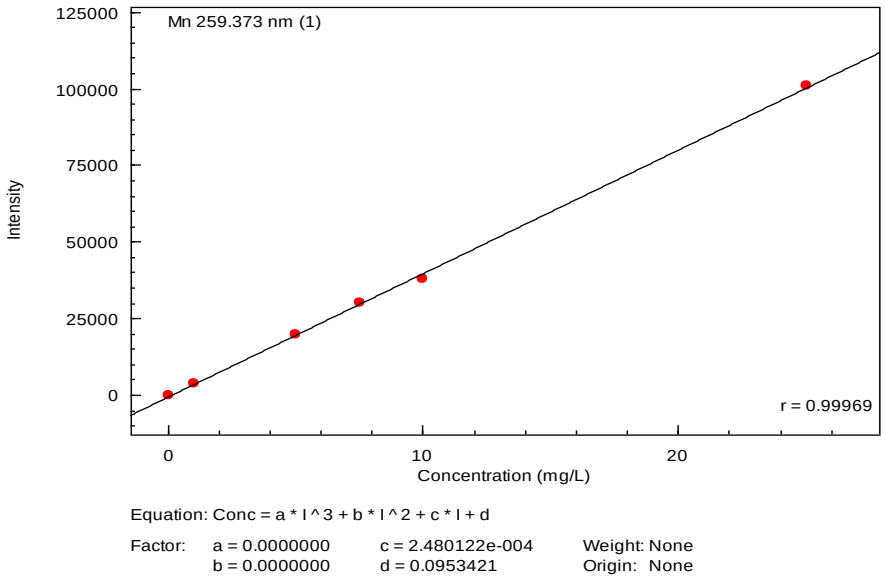

Figure A1. ICP OES calibration curve

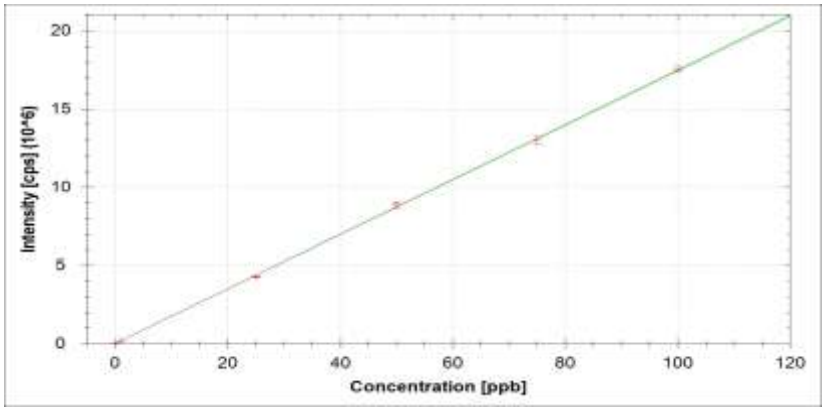

f(x) = 174527.6811*x + 14732.0477
R_2 = 0.9998
BEC = 0.084 ppb
LoD = 0.0064 ppb

Figure A2. I CAP Q ICP MS calibration curve

Table A1. Comparative test between two analytical instruments

Sample No	ICAP Q ICP MS mg/L	OES ICP mg/L
QA1	4.967	5.012
QA2	15.106	15.365
QA3	24.934	25.003

APPENDIX B

Table B1. Effects of adsorbent dosage on Zn removal

	Zn
Adsorbent dosage(mg)	% Removal
1200	78.831
1000	72.229
800	62.977
600	51.056
400	33.788
200	18.001

Table B2. Effects of adsorbent dosage on Cu removal

	Cu
Adsorbent dosage(mg)	% Removal
1200	72.359
1000	66.723
800	56.359
600	44.861
400	30.659
200	17.247

Table B3. Effects of adsorbent dosage on Mn removal

	Mn
Adsorbent dosage(mg)	% Removal
1200	73.483
1000	64.818
800	53.999
600	42.640
400	33.537
200	15.763

Table B4. Effects of adsorption time on removal of Zn, Cu and Mn

	Ce, (mg/l). Difference between two experimental sets in brackets		
Time(min)	Zn	Cu	Mn
0	43.925 (0.000)	43.506 (0.000)	43.395 (0.000)
5	22.579 (0.086)	25.50 (0.738)	28.050 (0.268)
10	18.152 (0.064)	20.272 (0.226)	25.501 (0.051)
20	15.757 (0.023)	17.82 (0.502))	23.97 (0.477)
30	13.116 (0.112)	15.305 (0.190)	21.500 (0.020)
45	12.446 (0.014)	12.475 (0.443)	20.556 (0.422)
60	12.455 (0.001)	11.767 (0.114)	17.051 (1.004)
180	12.198 (0.164)	12.025 (0.001)	15.267 (0.718)
1440	12.152 (0.156)	10.923 (0.282)	15.861 (0.296)

Table B5. Effects of particle size on removal of Zn, Cu and Mn

	Ce, (mg/L). Difference between two experimental sets in brackets		
Particle size(mm)	Zn	Cu	Mn
0.15	11.175(0.227)	9.175(0.341)	12.110(0.266)
0.4	12.298(0.157)	14.478(0.441)	15.267(0.718)
1	20.928(0.125)	22.454(0.128)	34.901(0.899)
5	36.768(0.597)	36.673(0.223)	41.012(0.172)

Table B6. Effects of Initial concentration on adsorption of Zn, Cu and Mn

	Zn	
Ideal Initial Conc(mg/L)	Actual Initial Conc(mg/L)	Percentage removal
25	23.983	73.434
50	43.925	71.248
80	77.344	62.453
100	94.871	67.745

	Cu	
Ideal Initial Conc(mg/L)	Actual Initial Conc(mg/L)	Percentage removal
25	23.459	58.513
50	43.506	66.723
80	77.716	59.084
100	91.099	61.569

	Mn	
Ideal Initial Conc(mg/L)	Actual Initial Conc(mg/L)	Percentage removal
25	24.087	60.163
50	46.895	62.607
80	78.049	46.261
100	95.466	43.143

Table B7. Selectivity of the banana peel powder

Metal ion	Ternary component solution	Single component solution
	Percentage removal	Percentage removal
Metals		
Zn	50.993	72.34
Cu	54.963	66.97
Mn	35.074	62.61

Table B8. Effects of pH on adsorption Zn, Cu and Mn.

	Zn
pH	% Removal
2	42.354
3	72.684
5	80.386
	Cu
pH	% Removal
2	34.648
3	66.723
5	66.02
	Mn
pH	% Removal
2	28.237
3	62.607
5	72.121

Table B9. Langmuir and Freundlich isotherm data

Zn

Mass(mg)	Ce	Co	X	x/m=qe	1/Ce	1/qe	logCe	Log qe
200	36.016	43.925	1.5818	7.909	0.027765	0.126438	1.556495	0.898121576
400	29.084	43.925	2.9682	7.4205	0.034383	0.134762	1.463654	0.870433169
600	21.499	43.925	4.4852	7.475333	0.046514	0.133773	1.332418	0.873630563
800	16.262	43.925	5.5326	6.91575	0.061493	0.144597	1.211174	0.839839285
1000	12.198	43.925	6.3454	6.3454	0.081981	0.157594	1.086289	0.802459004
1200	9.299	43.925	6.9252	5.771	0.107538	0.17328	0.968436	0.761251074

Cu

Mass(g)	Ce	Co	X	x/m=qe	1/Ce	1/qe	logCe	Log qe
200	36.003	43.506	1.5006	7.503	0.027775	0.13328	1.556339	0.875234946
400	30.178	43.506	2.6656	6.664	0.033137	0.15006	1.47969	0.823734988
600	23.991	43.506	3.903	6.505	0.041682	0.153728	1.380048	0.813247301
800	18.998	43.506	4.9016	6.127	0.052637	0.163212	1.278708	0.78724788
1000	14.478	43.506	5.8056	5.8056	0.06907	0.172247	1.160709	0.76384711
1200	12.009	43.506	6.2994	5.2495	0.083271	0.190494	1.079507	0.72011794

Mn

Mass(g)	Ce	Co	X	x/m=qe	1/Ce	1/qe	logCe	Log qe
200	37.013	43.395	1.2764	6.382	0.027018	0.156691	1.568354	0.8049568
400	31.178	43.395	2.4434	6.1085	0.032074	0.163706	1.493848	0.785934578
600	24.891	43.395	3.7008	6.168	0.040175	0.162127	1.396042	0.790144365
800	19.962	43.395	4.6866	5.85825	0.050095	0.170699	1.300204	0.767767901
1000	15.227	43.395	5.6336	5.6336	0.065673	0.177506	1.182614	0.750786008
1200	11.505	43.395	6.378	5.315	0.086919	0.188147	1.060887	0.725503269

Table B10. Adsorption data on column studies at 6cm bed depth

			Mn	Zn	
	Actual AMD	Initial Conc(mg/L):	46.003	3.505	
	Flow: 15 ml/min	**Depth: 6 cm**			
Time	Sample No	**Ce**	**Ce/Co**	**Ce**	**Ce/Co**
3	3-10g-F15	0.0079	0.000172	0.0021	0.000599144
5	5-10log-F15	0.0182	0.000396	0.002	0.000570613
8	8-10log-F15	0.069	0.0015	0.003	0.00085592
10	10-10g-F15	0.096	0.002087	0.005	0.001426534
15	15-10g-F15	4.978	0.108203	0.067	0.019115549
20	20-10g-F15	11.156	0.24249	0.098	0.027960057
25	25-10g-F15	26.845	0.583511	0.12	0.034236805
35	35-10g-F15	45.351	0.985763	0.149	0.042510699
60	60-10g-F15	44.987	0.977851	1.485	0.423680456
75	75-10g-F15	45.86	0.996827	2.821	0.804850214
90	90-10g-F15	45.911	0.997935	2.731	0.779172611
120	120-1og-F15	46.211	1.004456	3.409	0.972610556
135	135-10g-F15	46.008	1.000043	3.528	1.006562054
150	150-10g-F15	46.015	1.000196	3.487	0.994864479
180	180-10g-F15	46.013	1.000152	3.507	1.000570613

Table B11. Data on column studies on 12.4 cm bed depth

			Mn	Zn	
	Actual AMD	Initial Conc(mg/L)	46.003	3.505	
	Flow: 15 ml/min	Depth: **12.4 cm**			
Time	Sample No	**Ce**	**Ce/Co**	**Ce**	**Ce/Co**
3	3-20g-F15	0.007	0.000152154	0.002	0.000570613
5	5-20log-F15	0.044	0.000956397	0.002	0.000570613
8	8-20log-F15	0.052	0.001130287	0.001	0.000285307
10	10-20g-F15	0.0651	0.001415033	0.003	0.00085592
15	15-20g-F15	0.082	0.001782376	0.002	0.000570613
20	20-20g-F15	0.089	0.00193453	0.029	0.008273894
25	25-20g-F15	0.127	0.002760509	0.046	0.013124108
35	35-20g-F15	24.342	0.529104899	0.088	0.02510699
60	60-20g-F15	39.991	0.869256184	0.226	0.064479315
75	75-20g-F15	41.235	0.896296135	0.889	0.25363766
90	90-20g-F15	42.971	0.934030344	1.893	0.540085592
120	120-20g-F15	44.883	0.97559014	2.657	0.758059914
135	135-20g-F15	45.671	0.992718341	3.267	0.932097004
150	150-20g-F15	45.979	0.99941312	3.56	1.015691869
180	180-20g-F15	46.002	0.999913055	3.508	1.00085592

Table B12. Data on column studies on 17.8 cm bed depth.

				Mn		Zn	
		Actual AMD	Initial Conc(mg/L):		46.003	3.505	
		Flow: 15 ml/min	Depth: **17.8 cm**				
Time	Sample No		**Ce**	**Ce/Co**		**Ce**	**Ce/Co**
3	3-30g-F15	0.00254	5.52102E-05	0	0		0
5	5-30log-F15	0.0067	0.000145633	0	0		0
8	8-30log-F15	0.015	0.000326044		0.001	0.000285307	
10	10-30g-F15	0.019	0.00041299	0	0.001	0.000285307	
15	15-30g-F15	0.024	0.000521671	0	0.001	0.000285307	
20	20-30g-F15	0.019	0.00041299	0	0.003	0.00085592	
25	25-30g-F15	0.0131	0.000284745	0	0.005	0.001426534	
35	35-30g-F15	0.12	0.002608355	0	0.086	0.024536377	
60	60-30g-F15	23.696	0.515063253	0	0.101	0.028815977	
75	75-30g-F15	29.258	0.635960527	0	0.256	0.073038516	
90	90-30g-F15	36.597	0.795483198	0	0.337	0.096148359	
120	120-30g-F15	42.775	0.92977003	0	1.994	0.568901569	
135	135-30g-F15	44.785	0.973459983	0	3.312	0.944935806	
150	150-30g-F15	46.031	1.000543407	0	3.488	0.995149786	
180	180-30g-F15	46.021	1.000326044	0	3.501	0.998858773	

Table B13. Data on column studies at 30 mL/min.

			Mn		Zn	
	Actual AMD	Initial Conc(mg/L):		46.003	3.505	Actual AMD
	Flow: **30mL/min**	Depth: 17.4 cm				
Time	**Sample No**	**Ce**	**Ce/Co**	**Ce**		**Ce/Co**
3	3-30g-F30	0.007	0.000152	0		0
5	5-30log-F30	0.039	0.000848	0		0
8	8-log-F30	0.0511	0.001111	0		0
10	10-30g-F30	0.084	0.001826	0.001		0.000285307
15	15-30g-F30	0.119	0.002587	0.006		0.00171184
20	20-30g-F30	1.468	0.031909	0.049		0.013980029
25	25-30g-F30	4.338	0.094292	0.098		0.027960057
35	35-30g-F30	19.294	0.41938	0.104		0.029671897
60	60-30g-F30	40.088	0.871365	0.265		0.075606277
75	75-30log-F30	42.898	0.932444	0.443		0.12639087
90	90-30g-F30	44.358	0.964179	0.952		0.271611983
120	120-30g-F30	45.182	0.982089	2.921		0.833380884
135	135-30g-F30	45.819	0.995935	3.608		1.029386591
150	150-30g-F30	46.016	1.000217	3.5		0.998573466
180	180-30g-F30	46.009	1.000065	3.501		0.998858773

Table B14 Data on column studies at 45 mL/min

			Mn	Zn	
	Actual AMD	Initial Conc(mg/L)	46.003	3.505	
	Flow: **45 ml/min**	Depth: 17.8 cm			
Time	**Sample No**	**Mn**	**Ce/Co**	**Ce**	**Ce/Co**
3	3-30g-F45	0.01	0.000217363	0	0
5	5-30log-F45	0.114	0.002477938	0	0
8	8-30log-F45	0.484	0.010520367	0.0079	0.00225392
10	10-30g-F45	0.986	0.021431987	0.021	0.00599144
15	15-30g-F45	7.434	0.161587619	0.08	0.02282454
20	20-30g-F45	16.158	0.351215059	0.298	0.0850214
25	25-30g-F45	22.123	0.48087206	0.489	0.13951498
35	35-30g-F45	38.034	0.826718254	1.743	0.49728959
60	60-30g-F45	42.832	0.931008999	2.689	0.76718973
75	75-30g-F45	44.934	0.976698691	3.41	0.97289586
90	90-30g-F45	46.004	0.999956527	3.426	0.97746077
120	120-30g-F45	46.016	1.000217363	3.487	0.99486448
135	135-30g-F45	46.148	1.003086554	3.502	0.99914408
150	150-30g-F45	46.062	1.001217233	3.49	0.9957204
180	180-30g-F45	46.022	1.000347781	3.508	1.00085592

Table B15. The residual ions and the percentage removed by adsorption on the banana peel powder from the fortified AMD.

	Zn		Cu		Mn		Co		Fe		Ni		Cd		Al	
Dose, mg	Final Conc	% Rem	Final Conc	% Rem	Final Conc	% Rem	Final Conc	% Rem	Final Conc	% Remo	Final Conc	% Remo	Final Conc	% Rem	Final Conc	% Removal
	mg/L	mg/L		mg/L		mg/L		mg/L		mg/L		mg/L			mg/L	
0	33.92	0	46.60	0	46.00	0	3.18	0	6.102	0	3.75	0	0.35	0	15.12	0
200	32.70	3.60	23.87	48.79	35.51	22.82	2.61	18.07	0	100	3.10	17.35	0.00	98.71	6.73	55.50
400	26.70	21.31	20.06	56.96	32.73	28.86	2.56	19.36	0	100	3.03	19.20	0.00	98.71	6.00	60.32
600	26.13	22.98	21.28	54.33	34.02	26.06	2.65	16.78	0	100	3.06	18.27	0.00	99.29	5.45	63.98
800	22.36	34.07	16.14	65.35	31.60	31.32	2.53	20.42	0	100	2.95	21.40	0.00	99.29	4.32	71.41
1000	19.94	41.21	15.03	67.74	32.43	29.52	2.48	22.05	0	100	2.88	23.02	0.00	99.29	3.07	79.73
1200	18.31	46.02	13.80	70.38	31.80	30.90	2.43	23.49	0	100	2.91	22.47	0.00	99.57	2.94	80.59

Table B16. The residual ions and the percentage removed by adsorption on the banana peel powder from the actual AMD.

	Zn		Cu		Mn		Co		Fe		Ni		Cd		Al	
Dose, mg	Final Conc mg/l	% Rem	Final Conc mg/l	% Rem	Final Conc mg/l	% Rem	Final Conc mg/l	% Rem	Final Conc mg/l	% Rem	Final Conc mg/l	% Remo	Final Conc mg/l	% Rem	Final Conc mg/l	% Removal
0	3.51	0	0	0	46.00	01	3.18	0	6.102	0	3.75	0	0.35	0	15.12	0
200	1.68	52.13	0	0	40.24	12.54	2.505	21.21	0	100	1.12	70.19	0.00	99.71	4.23	72.00
400	1.22	65.14	0	0	34.12	25.85	2.36	25.65	0	100	0.93	75.25	0.00	0	2.16	85.75
600	0.93	73.44	0	0	28.9	37.19	2.14	32.82	0	100	0.03	99.08	0.00	0	.83	94.53
800	0.74	78.86	0	0	19.87	56.81	2.00	37.00	0	100	0.02	99.6	0.00	0	.08	99.47
1000	0.69	80.34	0	0	9.635	79.06	1.83	42.41	0	100	0.01	99.71	0.00	0	0	100
1200	0.331	90.56	0	0	5.86	87.86	57.6	57.6	0	100	0	100	0.00	0	0	100